Available online at www.sciencedirect.com

ScienceDirect

Applied Energy 00 (2019) 1–19

Applied Energy

An Integrated Framework for Sizing and Energy Management of Hybrid Energy Systems Using Finite Automata

Yara Khawaja[a*], Adib Allahham[a], Damian Giaouris[a], Charalampos Patsios[a], Sara Walker[a], and Issa Qiqieh[b]

[a] *School of Engineering, Newcastle University, Newcastle upon Tyne, NE1 7RU, UK*

[b] *Faculty of Engineering. Al-Balqa' Applied University, Al-Salt, Jordan*

Abstract

Due to the significance of hybrid energy systems, selecting the appropriate sizing-energy management strategy combination represents a key factor to ensure the efficient operation while offering a competitive operating cost. This paper presents an integrated framework for finding the best size-energy management strategy combination for a hybrid energy system. Fundamental to this framework is utilizing finite automata to develop multiple energy management strategies that fully take into consideration the dynamic relationship between all the assets in the hybrid energy system. The proposed integrated framework consists of three main steps. First, an analytical and economic sizing approach is performed to find the initial sizes of the hybrid energy system assets based on an initial energy management strategy; second, using finite automata to implement the initial energy management strategy and instantiate different energy management strategies; and third, an evaluation model is developed to assess the instantiated energy management strategies and extract the featured conditions to create new-improved one. This new energy management strategy is used to re-exercise the analytical and economic sizing to obtain the best size-energy management strategy combination. The novelty in this work can be summarized as taking the impact of selecting the right energy management strategy on the sizing of a hybrid energy management. This can lead to better performance and can be explained in our integrated framework by reducing the cost, reducing the diesel generator and fuel cell working hours and increasing the photovoltaic utilization. Moreover, using finite automata in implementing and instantiating multiple energy management strategies to attain an improved one has not been reported. A comparison between the results of the proposed framework and the results of the analytical and economic sizing approach is carried out. The size of the photovoltaic is reduced from 140 kW to 60 kW when using the integrated framework and therefore the size of the electrolyzer and the hydrogen tank reduced to the half. Moreover, a reduction in the diesel generator working hours by 35% and in the levelized cost of energy by 40% are achieved.

Keywords: Hybrid energy systems, Energy management strategies, Finite Automata, Analytical and Economical Sizing, Integrated Framework.

1. Introduction

In recent decades, there has been a considerable growth in the installed capacity of renewable and alternative energy technologies. These technologies include energy generation from renewable energy (RE) resources (*e.g.*, photovoltaics (PVs),concentrated solar power plants (CSP), wind turbines (WTs)), and alternative energy (AE) resources (*e.g.*, fuel cells (FCs) and microturbines (MTs)) [1, 2, 3, 4, 5]. The key drivers for the deployment of the above resources are their benefits in reducing carbon emissions and ensuring sufficient supply to satisfy demand at all times [5, 6]. However, the intermittent characteristics of such resources gives the motivation to design and construct the hybrid energy systems (HESs).

A HES combines two or more of RE/AE and conventional energy sources along with an energy storage system [7, 4]. The main role of the HES is to ensure the maximum production of energy while maintaining the quality of the supplied service [8]. HES considered the most attractive option where grid connectivity is practically impossible or uneconomical [9], especially for power generation in remote areas [3].

On the environmental level, HESs can reduce the emissions of greenhouse gas through the increased use of REs [10]. Also it has been demonstrated that HESs can significantly reduce the total life-cycle cost of standalone systems in many situations, while at the same time providing a more reliable supply of electricity [4], [11].

In order to obtain the best performance of HESs in terms of maximizing the utilization of the generated energy and minimizing the total cost, two crucial issues are considered: appropriate sizing and suitable energy management strategy [12], [13], [14], [15].

*Corresponding author

Email address: y.khawaja2@newcastle.ac.uk (Yara Khawaja[a*])

Nomenclature

β	temperature coefficient of solar cell efficiency, 1/°C
η_{ch}	battery charge efficiency
η_{dch}	battery discharge efficiency
η_{inv}	inverter efficiency
η_{module}	PV module efficiency
η_{PV}	PV overall efficiency
η_{sys}	system overall efficiency
η_{temp}	PV temperature efficiency
A, B	diesel generator consumption curve coefficients, L/kWh
A_{PV}	PV total area, m^2
B_{DSL}	binary logic for diesel generator operation
B_{EL}	binary logic for electrolyzer operation
B_{FC}	binary logic for fuel cell operation
Bat_C	battery capacity, kWh
C_{Bat}	total cost of battery energy system, £
$C_{BES,OM}$	O&M cost for battery, £/kWh
$C_{DSL,fuel}$	diesel generator total fuel cost, £/L
$C_{DSL,OM}$	O&M cost for diesel generator, £/kW
C_{DSL}	total cost of diesel generator, £
$C_{inv,OM}$	O&M cost for inverter, £/kW
$C_{inv,PV}$	total cost of PV inverter, £
$C_{PV,OM}$	O&M cost for PV, £/kW
$DE(n)$	deficiency in energy supplied to the load
DEG_{BES}	battery energy system degradation rate
DEG_{PV}	PV degradation rate
E_{BES}	energy produced by the BES, kWh
E_{DSL}	energy produced by the diesel generator, kWh
E_{PV}	energy produced by PV, kWh
E_{system}	total energy of the HES, kWh
F	Faraday constant, C/mol
F_{consum}	diesel generator fuel consumption, L
f_p	fuel unit cost, £/L
H	yearly module reference in-plane radiation, kW/m^2
$H_{2,cons,1kW}$	H_2 consumed by 1 kW fuel cell in 1 h, mol/h
$H_{2,prod,1kW}$	H_2 produced by 1 kW electrolyzer in 1 h, mol/h
HA	battery hours of autonomy, hrs
HA_{H_2}	hydrogen tank hours of autonomy, hrs
I_{NOCT}	solar radiation at NOCT, W/m^2
I_{PV}	solar radiation, kW/m^2
IC_{BES}	initial cost for battery, £/kWh
IC_{DSL}	initial cost for diesel generator, £/kW
IC_{inv}	initial cost for inverter, £/kW
IC_{PV}	initial cost for PV, £/kW
j	index of year
$LCOE$	levelized cost of energy, £/kWh
LHV	low heat value of hydrogen, kWh/kg
$Life_{DSL,h}$	life time of diesel generators, hrs
$Life_{DSL}$	life time of diesel generators, years
M_{DSL}	diesel generator margin coefficient
M_{FC}	fuel cell margin coefficient
N	hybrid energy system lifetime, years
n	index of hours in a year
$NOCT$	normal operating cell temperature, °C
$P_{DSL,rated}$	diesel generator rated power, kW
$P_{DSL}(n)$	hourly generated power by diesel generator, kW
$P_{EL,min}$	electrolyzer minimum power, kw
$P_{EL,rated}$	electrolyzer rated power, kw
$P_{EL}(n)$	hourly power consumed by electrolyzer, kW
$P_{FC,rated}$	fuel cell rated power, kW
$P_{FC}(n)$	hourly power generated by fuel cell, kW
P_{HT}	hydrogen tank final pressure, bar
$P_{input}(n)$	sum of input power to battery at a specific hour, kW
$P_{PV,rated}$	PV rated power, kW
$P_{PV,surplus}$	surplus power generated from PV
$P_{PV}(n)$	hourly power generated by PV, kW
$PL(n)$	hourly load, kW
PL_{avg}	average hourly load, kW
PL_{max}	maximum load, kW
r	discount rate
RC_{BES}	replacement cost for battery, £/kWh
RC_{DSL}	replacement cost for diesel generator, £/kW
RC_{inv}	replacement cost for inverter, £/kW
S_{HT}	hydrogen tank size, kg
SFC	specific fuel consumption for diesel generator, L/kWh
soc	battery state of charge
soc_{DSL}	battery soc for diesel generator operation
soc_{FC}	battery soc for fuel cell operation
soc_{max}	maximum battery state of charge
soc_{min}	minimum battery state of charge
$socHT$	Hydrogen tank state of charge
$socHT_{max}$	maximum hydrogen tank state of charge
$socHT_{min}$	minimum hydrogen tank state of charge
$T_{amb,NOCT}$	ambient temperature of NOCT, °C
T_{amb}	ambient temperature, °C
T_{cell}	PV cell temperature, °C
T_{ref}	PV cell reference temperature, °C
V_{el}	electrolyzer working voltage, volt
V_{FC}	fuel cell working voltage, volt
WH_{DSL}	yearly working hours of diesel generator, hrs
WH_{EL}	yearly working hours of electrolyzer, hrs
WH_{FC}	yearly working hours of fuel cell, hrs
BES	battery energy system
DOD	battery depth of discharge
DSL	diesel generator
EL	electrolyzer
EMS	energy management strategy
FA	finite automata
FC	fuel cell
HES	hybrid energy system
HT	hydrogen tank
LPSP	loss of power supply probability
PV	photovoltaic

The literature can be classified into three research directions: (i) finding the optimal size of HES based on a given EMS, (ii) obtaining the optimal EMS of a fixed size HES, and (iii) optimizing the size and EMS of HES.

In the literature, finding the optimal size of a HES can be classified into probabilistic, analytical, iterative, artificial intelligence (AI) and hybrid methods [16]. For instance, Li et al. [17] presented a size optimization method for three standalone HESs with hydrogen system. An analytical technique is used to find the energy balance throughout the year and a trade-off between maximum system efficiency and minimum system cost.

While Smaoui et al. [18] applied an iterative technique, to find the optimal size of a standalone PV/wind/hydrogen system HES supplying a desalination unit. The algorithm gives all possible configurations that can completely cover the freshwater requirements of isolated consumers. The optimal configuration is chosen based on the minimum initial cost. Whereas Maleki et al. [19] provided a comparative study to evaluate the performance of different AI techniques for optimum sizing of a PV/wind/Fuel cell hybrid system to continuously satisfy the load with the minimal total cost. Four heuristic algorithms, namely, particle swarm optimization, tabu search, simulated annealing, and harmony search, are applied to the HES. The optimal size is determined based on the minimum total annual cost. Amrollahi et al. in [20] modeled the components of the hybrid PV/WT/battery mathematically within the framework of the integer linear programming method. Two cases with and without applying the demand side program were extracted and compared with each other then the optimum configuration was determined.

Various EMSs are developed to ensure the optimal operation of a HES. For example, Torreglosa et al. [21] introduced an EMS for standalone PV/WT/battery/hydrogen system HES. This EMS is formed in a hierarchical control composed by a master and a slave control strategy. Lin et al. in [22] proposed an EMS for microgrid using enhanced bee colony optimization technique. The proposed EMS aims at minimizing the operating cost of the HES. While Luna et al. implemented an EMS based on mixed-integer linear programming, that allows to reduce cost in the HES and also can include technical restriction for managing the storage devices in a proper way [23].

On the other hand, combining both optimal size and EMS of a HES leads to achieve more reliable design, by incorporating the best features from the optimal sizing together with the optimal operation of the HES. Zhao et al. [24] presented an optimal sizing and operating strategy to design a PV/WT/BES/Diesel HES on Dongfushan Island, China. The EMS operates under three unique modes based on the coordination of energy storage. Combined with the EMS, a genetic algorithm is used to solve the sizing optimization problem to ensure cost minimization, maximal RE generation, and pollutant emission minimization. However, the proposed EMS was optimized based on the energy storage alone neglecting the effect of all other components on the EMS. A sizing method based on Simulink design optimization of a standalone PV/BES/Hydrogen system HES is employed in [25]. In addition three control strategies based on technical-economic aspects are considered for the EMS. The right configuration, sizing, and EMS are found using a dynamic model of the HES. The optimization was done only to satisfy load and maintain a certain level at the hydrogen tank and the battery's state of charge, with simple total cost calculations. In [26] an optimal sizing and EMS of PV/WT/hydrogen system HES are presented. The objective of HES optimal designing is defined as the total net present cost minimization considering reliability indices improvement as values of loss of energy expected and loss of load expected. A new meta-heuristic nature-inspired algorithm called flower pollination algorithm is used for the optimal design. However, the studied HES considered only RE resources and hydrogen system as a storage which has low energy density, and there is no backup generation.

The main objective of the above studies is to obtain the optimal size, optimal EMS or both, which is also the main aim of our work. However, the existing approaches that addressed the optimal size and EMS of a HES did not take into consideration the impact of choosing an appropriate EMS on the assets' sizing. Taking the impact of selecting the right EMS can lead to better performance of the HES. This is can be explained in our integrated framework by reducing the cost of the HES, reducing the diesel generator and fuel cell working hours and increasing the PV utilization. Moreover, using FA in implementing and instantiating multiple EMSs to attain an improved EMS has not been reported. Modeling the EMSs using FA has many advantages in terms of reducing the complexity of the system, better understanding of the HES, facilitate the adding or changing of the operating conditions and increasing the ability to accommodate new subsystems (Section 2.2). At this point it can be stated that another approach could have used with similar results, i.e. start from an initial EMS, use FA to generate multiple EMSs, and then find the optimum size for each EMS and finally choose the most suitable combination of size-EMS. However this would not result in a more efficient system as the initial derivation of the most suitable EMS would have to take place in a system that is not optimally sized.

In this paper, we propose an integrated framework to find the optimal size-EMS combination for a standalone HES. In the first step, the proposed framework finds the size of the HES based on an initial EMS and input data. Then the obtained size is exercised through multiple EMSs, which are produced using Finite Automata (FA). The application of FA will facilitate the process of developing and instantiating EMSs by modifying the operating conditions of the assets in the HES. This is followed by an evaluation model to compare the performance indices of each instantiated EMS. The performance indices adopted in this study are diesel generator, fuel cell and electrolyzer working hours, levelized cost of energy, fuel cost, and PV contribution. The role of the evaluation model is to track the featured conditions that lead to improvement in performance indices and retain them in the new EMS. As such, the new-optimized EMS will then replace the initial one leading to the optimal size-EMS combination. This study further explores the significance of minimizing the excess energy from the HES to reduce the cost of HES components. The main contributions of this work can

be summarized as follows:

1. We propose an integrated framework to find the optimal size-EMS combination of a standalone hybrid PV/BES/diesel/hydrogen system.
2. We leverage Finite Automata to implement and instantiate multiple EMSs to reduce the resulting redundancy when using if-else statements for the EMS representation.
3. We address the impact of choosing the right EMS on the HES assets' sizing and cost reduction.

To the best of our knowledge, this is the *first* demonstration of a integrated framework for finding the optimal size-EMS combination of a standalone HES using FA. The rest of the paper is organized as follows. Section 2 explains the architecture of the HES under study and how to model it in FA. Section 3 introduces the AES approach which is the first step in the proposed integrated framework. Section 4 describes the proposed integrated framework. Results and discussion are described in Section 5. Finally, Section 6 concludes the paper.

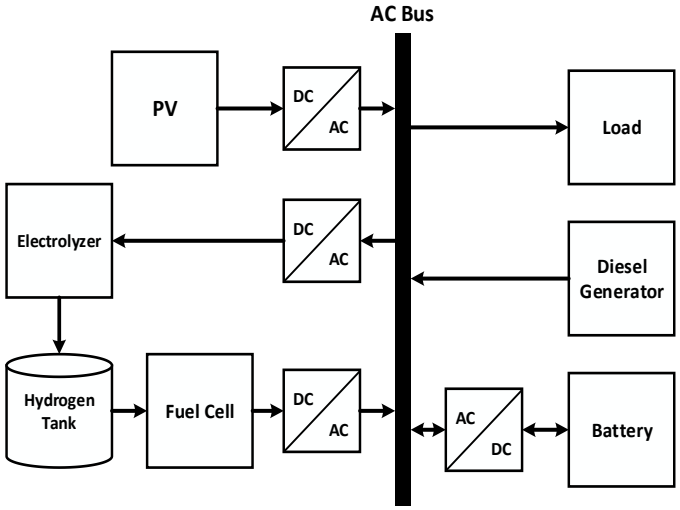

Figure 1: Hybrid energy system network diagram. The system consist of PV, BES, diesel generator, electrolyzer, fuel cell, hydrogen tank and load.

2. Hybrid Energy System Structure and Modeling in Finite Automata

This section introduces the architecture of the HES, background on FA and explaining a simple BES example in FA, and finally, the implementation of the initial EMS in FA is explained in detail.

2.1. HES Architecture

A simplified scheme of standalone HES is reported in Fig.1. The HES includes PV, battery energy system (BES), electrolyzer (EL), fuel cell (FC), hydrogen tank (HT), and diesel generator (DSL). The energy generated from the PV used to supply the load and the surplus energy will be stored in the BES. Any further surplus PV energy is directed to the EL to produce hydrogen which will be stored in the HT. The BES state of charge (*soc*) will be checked continuously, there are two *soc* predefined levels that will determine the operating point of the FC and DSL. The first predefined level is soc_{FC} that when the BES *soc* reaches this value, the FC will start operating after checking if there is available H_2 in the HT. The second predefined level is soc_{DSL} when BES *soc* reaches or goes below this value, the DSL will start operating[1]. All the energy sources use DC/AC power inverters for connection to a common AC bus, which allows a suitable EMS. Although inverter efficiency is not constant in reality, in our model it is assumed to be constant.

2.2. Finite Automata

Discrete event systems (DES) are discrete-state, event-driven systems among a set of finite states, with an initial state and one or more of marked states. [27, 28]. Traditionally, regular languages and finite automata have been used both for modeling and analysis of discrete event systems in the supervisory control community [29].

The first application of DESs in power system was in 1995 where Prosser et al. [30] modeled a 14-bus 40-line transmission network using DES. Two states were considered for each line: line in service and line out of service. While the events that triggered the system are: line restoring and line tripping. The supervisory control of DES (SCDES) was designed to manage the restore operation of tripping lines with a high level of security. Similarly, Lee et al. applied SCDES to obtain the restoration strategies for the power distribution networks, while maintaining a high level of security and satisfaction of the load [31]. While Afzalian et al [32, 33] applied SCDES for the operation of the tap-changing transformer, and dynamic flow controllers. The components are modeled using Automata and synthesized using TCT software [34]. Whereas Kharrazi et al. [35] studied the application of SCDES to a custom power park (CPP). The components in CPP are modeled using Automata, synthesized using the TCT software and simulated using Matlab/Simulink. Recently, Sadid et al. presented the scheduling of thermal devices operation in the framework of DESs, by modeling and design of admission control to be carried out in a systematic manner and ensuring the existence of the feasible scheduling prior to exploring control solutions.

Modeling the HES using FA has many advantages: (i) reducing the complexity of the system by dividing it into smaller subsystems, (ii) making the control of each subsystem simpler, (iii) providing a graphical representation of the system for better understanding of the HES, (iv) reducing the computation time since the state transition for each subsystem is done in parallel, (v) providing an easier way to modify the predefined conditions or adding new conditions to the existing system, and (vi) increasing the ability to accommodate new subsystems.

To illustrate how a subsystem in HES can be treated as a DES and modeled in FA, an example of a BES is presented in Fig. 2. The BES in HES has four states: charging, discharging, idle

[1] In such systems, hysteresis zones are usually employed to avoid multiple switchings of the system's assets. Having said that, in this work we do not use them as they do not influence our analysis.

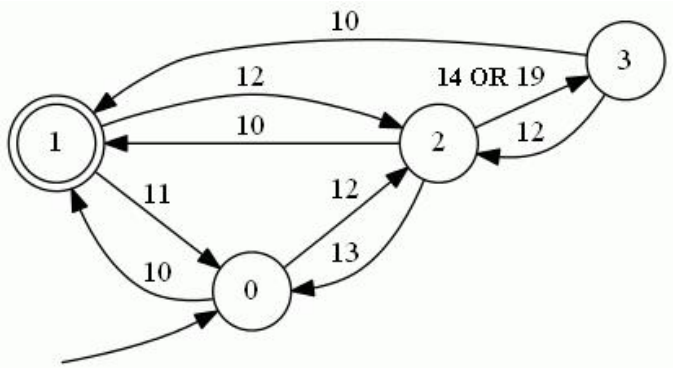

Figure 2: An illustrated example on implementing BES using FA.

and OFF. The circles in the figure represent the states, while the transitions are the events or the operating conditions. The state with double circles symbolizes the marked state, which is also the final state, that indicates the completion of BES operation. The states and the events are labeled by numbers, the numbers from 0-9 used for states and any number from 10 and above used for events. The description of the conditions can be found in Table 1. State 0 is the OFF state which is also the initial state, OFF state indicates that BES can be full (reaches soc_{max}) or empty (reaches soc_{min}). This is determined by the operating condition, if condition 11 is satisfied ($soc \geq soc_{max}$) then the BES is OFF because its full. Whereas when condition 13 is satisfied ($soc \leq soc_{min}$) it means the BES is empty. State 1 denotes that BES is in charging state and its also the desired state, the condition related to entering this state is 10, "$P_{input}(n) > PL(n)$ & $soc(n) < soc_{max}$", where $P_{input}(n)$ the sum of input power to the BES at that instance. The condition that can change the state of BES from state 1 (charging) to state 2 (discharging) is 12, "$P_{input}(n) < PL(n)$ & $soc(n) > soc_{DSL}$", while the condition "$soc \leq soc_{min}$" will change the state of BES from state 2 (discharging) to state 0 (OFF). State 3 is the idle state, the state where the $P_{input}(n)$ at that instance equal to the load, leading to entering the BES in idle (no charging or discharging). Conditions 14 or 19, which are responsible to operate the DSL or FC, transfers the BES into state 3 (idle). There is no condition which transfers BES from state 3 to 0 directly. Condition 12 will transfer BES from state 3 to 2 and condition 10 moves the BES state from 3 or 2 to 1. The behavior of any system modeled using FA is usually described by a regular language and can be found in [36].

2.3. Implementing EMS using Finite Automata

The EMS is the algorithm that controls the flow of energy generated from all the assets in the HES to guarantee the energy balance while satisfying the constraints of the system [37], [38], [39]. The EMS can be represented by a set of finite states. The HES switches between these states according to predefined operating conditions. EMS is modeled by FA in the graphical representation as illustrated in Fig. 4. This figure demonstrates the initial EMS that used in the analytical and economic sizing (explained in Section 3) to find the initial size of HES. Table 1 shows the states and the conditions of $EMS_{initial}$, it has nine states given in Fig. 3 and thirteen operating conditions demonstrated in Table 1. As mentioned in Section 2.2, BES has four states: OFF, charge, discharge and idle. The states of the DSL, FC and EL are ON and OFF. While the HT has three state: OFF (full or empty), charge and discharge. The PV is considered always ON even if the solar radiation is zero and the load is also ON as well. Each state of the HES in Fig. 3 combines the states of subsystems and identifies the status of the HES at each time-step in the year. For instance, state 0 shows the BES is discharging while all the other subsystems are OFF and HT is empty. While state 1 indicates the BES is idle, DSL is ON and the rest of subsystems are OFF.

Figure 4 describes the implementation of $EMS_{initial}$ using FA that is used to instantiate different EMSs. State 0 is the initial state and state 2 is the marked state, the desired state that the HES is expected to complete its task at. In the first hour of the year, all the subsystems will be OFF except the BES (with the assumption it is full at the beginning of the simulation) which is discharging to supply the load. During each hour, the power generated from the PV, DSL, FC is calculated to find the hourly P_{input}. The BES state of charge soc and HT state of charge $socHT$ is also computed hourly. All these values are used in determining the binary values of DSL, FC, and EL. These binary values are used in the operating conditions to determine the next state of the HES. For example, condition 12 $P_{input}(n) < PL(n)$ & $soc(n) > soc_{DSL}$ keeps the HES in state 0 where all assets (other than the PV) are OFF and the BES is discharging. The occurrence of condition 10 and 17 are related to the surplus of P_{input} to supply the load, but with an insufficient surplus to generate H_2. Thus moves the HES from state 0 to state 8 where the BES is in charging state and all the other assets (other than the PV) are in OFF state. Condition 14 leads to the operation of the DSL, transferring the HES into state 1. The occurrence of condition 13 moves the system to state 3. In state 3 the DSL and the PV are the only assets operating, while the $socHT$ and soc are minimum. Condition 19 is related to FC operation which transfers the HES into state 4 where the BES is in idle mode, and HT is discharging. Returning from state 4 to 0 is linked to the occurrence of condition 20 when the HT is empty. In the same manner, we can track all the transitions between states.

3. Analytical and Economic Modeling of HES

The analytical and economical sizing approach (AES) performed in this work follows the same calculation steps reported in earlier work by the authors, as documented in [40]. A major difference between this work and [40] is that the system in [40] was grid connected while our HES here is not. Therefore, the methodology presented in [40] needs to be modified accordingly. This modification is presented in this section.

An optimization approach is used to determine the size of the PV and BES by iteratively changing the PV rated power from (0 - $\alpha \cdot PL_{max}$) kW with a step of 10 kW each time, where α is a constant equal to 10 and chosen to ensure the selected range will cover all possible PV sizes. PL_{max} in this study is 26.7 kW (residential load for 40 houses [41], Fig. 7), and therefore,

State 0	State 1	State 2
PV: ON Load: ON BES: discharge DSL: OFF EL: OFF FC: OFF HT: OFF (empty)	PV: ON Load: ON BES: idle DSL: ON EL: OFF FC: OFF HT: OFF (empty)	PV: ON Load: ON BES: charge DSL: OFF EL: ON FC: OFF HT: charge
State 3	**State 4**	**State 5**
PV: ON Load: ON BES: OFF (empty) DSL: ON EL: OFF FC: OFF HT: OFF (empty)	PV: ON Load: ON BES: idle DSL: OFF EL: OFF FC: ON HT: discharge	PV: ON Load: ON BES: OFF (full) DSL: OFF EL: ON FC: OFF HT: charge
State 6	**State 7**	**State 8**
PV: ON Load: ON BES: charge DSL: OFF EL: OFF FC: OFF HT: OFF (full)	PV: ON Load: ON BES: discharge DSL: OFF EL: OFF FC: OFF HT: OFF (full)	PV: ON Load: ON BES: charge DSL: OFF EL: OFF FC: OFF HT: OFF (empty)

Figure 3: Nine states that used to describe $EMS_{initial}$ based on FA.

Table 1: Operating conditions used for $EMS_{initial}$ operation.

Conditions	Description
10	$P_{input}(n) \geq PL(n)$ & $soc(n) < soc_{max}$
11	$soc(n) \geq soc_{max}$
12	$P_{input}(n) < PL(n)$ & $soc(n) > soc_{DSL}$
13	$soc(n) \leq soc_{min}$
14	$P_{input}(n) < PL(n)$ & $soc(n) \leq soc_{DSL}$ & $B_{FC} = 0$
15	$P_{input}(n) > PL(n)$
16	$P_{EL,min} \leq P_{PV,surplus}(n) \leq P_{EL,rated}$ & $socHT(n) < socHT_{max}$
17	$P_{PV,surplus}(n) < P_{EL,min}$
18	$socHT(n) \geq socHT_{max}$
19	$P_{input}(n) < PL(n)$ & $soc(n) \leq soc_{FC}$ & $socHT(n) > socHT_{min}$
20	$socHT(n) \leq socHT_{min}$

the range of PV rated power is selected (0 - 267) kW. A factor that determines the BES size is the hours of autonomy (HA), which means for how many hours a completely charged battery is able to supply the load continuously. Since the HES in this study is standalone, it is essential to choose a high value for HA. Therefore, HA is iteratively considered as 12, 24, 36, 48, and 60 hours. An EMS is employed here guarantees that the load is always supplied with energy and at the same time ensures the other assets of the system operate efficiently (1). The main idea is to generate multiple scenarios with different PV sizes and BES capacities, following that the levelized cost of energy (LCOE) is calculated for each scenario. The combination that provides the lowest LCOE while covering the load will be selected as the optimal solution.

$$PL(n) + P_{EL}(n) = P_{PV}(n) + P_{FC}(n) + P_{DSL}(n) \quad , \qquad (1)$$

where $P_{PV}(n)$, $P_{FC}(n)$, $P_{DSL}(n)$ are the hourly power generated by PV, FC and DSL respectively.

The method to calculate the LCOE and hence the optimum size of the system is shown in Fig. 5, while the models required for that process are presented in the following subsections. It is noted here that the assets that employ hydrogen are not included in the calculation of the LCOE, as the main focus of this work is not the LCOE (which has been done before). The flowchart in Fig. 5 summarizes the management rules to define, for each studied hour n, the electric energy flows through the system to supply the load. P_{pv-min} and P_{pv-max} are the minimum and maximum values in PV rated power range, soc is the state of charge of the battery, and k indicates the number of HA involved in this study. B_{FC}, B_{DSL}, B_{EL} are binary logic values for FC, DSL and EL computed hourly to identify which device is operating at that time.

This section presents both the analytical modeling for each component in the HES and the economic modeling used to compute the LCOE in assessing the system's economic profitability.

3.1. PV Analytical Modeling

The hourly output power P_{PV} produced by the PV arrays with an area A_{PV} is given by Eq. (2) [42], where I_{PV} is the total solar radiation onto one square metre in one hour, the solar radiation data for the city of Newcastle Upon Tyne [43] illustrated in fig. 6a is used in this study.

$$P_{PV}(n) = \begin{cases} I_{PV}(n) \cdot A_{PV} \cdot \eta_{pv}(n), & I_{PV}(n) \geq 0 \, . \\ 0, & I_{PV}(n) \leq 0 \, . \end{cases} \qquad (2)$$

The total area of PV arrays depends on the PV rated power and H the yearly module reference in-plane radiation (usually assumed to be 1000 W/m^2), and can be found using:

$$A_{PV} = P_{PV,rated}/(\eta_{module} \cdot H) \quad . \qquad (3)$$

The impact of temperature variations and PV degradation on the hourly PV overall efficiency $\eta_{PV}(n)$ and temperature efficiency $\eta_{temp}(n)$ is theoretically calculated by the following equations:

$$\eta_{PV}(n) = \eta_{module} \cdot \eta_{temp}(n) \cdot \eta_{inv} \cdot (1 - (N-1)DEG_{PV}) \quad , \quad (4)$$

$$\eta_{temp}(n) = [1 - \beta(T_{cell}(n) - T_{ref})] \quad , \qquad (5)$$

where $T_{cell}(n)$ is computed based on the hourly ambient temperature illustrated in Fig. 6a, $T_{amb}(n)$ illustrated in Fig. 6b, by:

$$T_{cell}(n) = T_{amb}(n) + [(NOCT - T_{amb,NOCT})/I_{NOCT}] \cdot I_{PV}(n) \quad . \quad (6)$$

The values of the technical parameters of PV are presented in Table2.

3.2. Battery Energy System Analytical Modeling

The power generated from the PV (Fig. 6) and the load profile (Fig. 7) at each time step, determine the charge or discharge energy flow from/to the BES and whether to operate the FC and DSL. The battery capacity Bat_C is calculated using Eq. (7) [40], [42], according to which the capacity of the

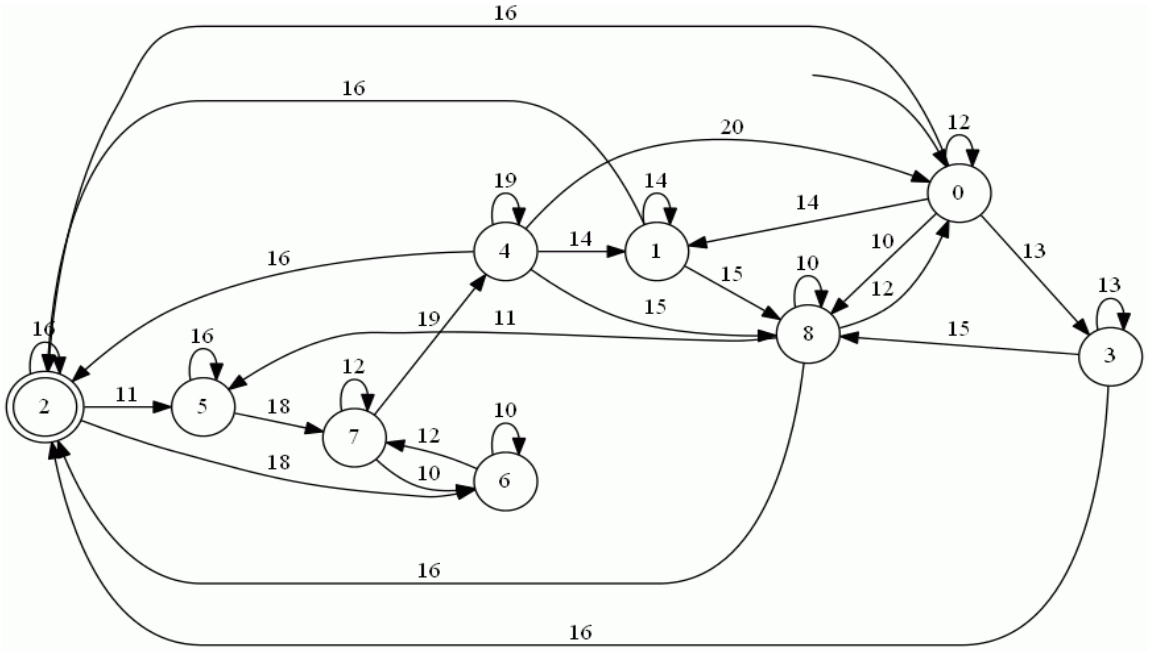

Figure 4: Implementing $EMS_{initial}$ in FA and using the states described in Fig. 3.

battery expressed in terms of HA and the average hourly demand PL_{avg}. $P_{L.avg}$, in our case, is equal to 10.7 kW, whereas HA ranges between five values, 12, 24, 36, 48, 60 hours.

$$Bat_C = \frac{HA \cdot PL_{avg}}{\eta_{inv} \cdot \eta_{ch} \cdot DOD} \quad , \tag{7}$$

where η_{inv} and η_{ch} are the inverter and BES charge efficiencies, and DOD is the depth of discharge. An important parameter to represent the available capacity in BES (expressed as a percentage of its rated capacity) is the state of charge (soc), which is used to decide whether to charge or discharge the BES. Depending on the renewable energy produced and the load power requirements, the hourly BES soc for charging and discharging modes can be calculated from Eq. (8), [42].

$$soc(n) = \begin{cases} soc(n-1) + \dfrac{[P_{input}(n) - PL(n)] \cdot \eta_{ch}}{\eta_{inv} \cdot Bat_C}, & P_{input}(n) > PL(n) \\ soc(n-1) - \dfrac{PL(n) - P_{input}(n)}{\eta_{inv} \cdot \eta_{dch} \cdot Bat_C}, & P_{input}(n) \leq PL(n), \end{cases} \tag{8}$$

where $soc(n)$ and $soc(n-1)$ are the states of charge of the BES at n and $n-1$ respectively, and η_{dch} is the discharging efficiency. $P_{input}(n)$ is the sum of input power to the BES at a specific hour and found using Eq. (9). If BES input power is greater than demand, $P_{input}(n) > PL(n)$, then the load will be supplied firstly and the surplus power will be used to charge BES. on the other hand, if $P_{input}(n) \leq PL(n)$, the power produced will be used to satisfy the load and any insufficiency will be covered by the BES.

$$P_{input}(n) = P_{PV}(n) + P_{DSL}(n) + P_{FC}(n) \quad . \tag{9}$$

To model an efficient power distribution system, BES soc should be maintained at a reasonable value between the two limit levels, soc_{max} and soc_{min} subject to the following constraint:

$$soc_{min} \leq soc(n) \leq soc_{max} \tag{10}$$

The parameters used in the BES analytical model are presented in Table. 3.

Table 2: Data used for PV analytical modeling [40, 44].

Parameter	Value
PV module efficiency, η_{module}	14%
PV degradation, DEG_{PV}	0.5%
PV cell reference temperature, T_{ref}	20 °C
Normal operating cell temperature, NOCT	45°C
Ambient temperature of NOCT, $T_{amb,NOCT}$	20°C
Solar radiation at NOCT, I_{NOCT}	800 W/m^2
Temperature coefficient of solar cell efficiency, β	0.005 1/°C
yearly module reference in-plane radiation, H	1000W/m^2
PV lifetime, N	20 years

Table 3: Data used for battery energy system analytical modeling [40].

Parameter	Value
Depth of discharge, DOD	80%
Charge efficiency, η_{ch}	80%
Discharge efficiency, η_{dch}	80%
Minimum state of charge, soc_{min}	20%
Maximum state of charge, soc_{max}	90%
Round trip efficiency, RT_{eff}	90%
Degradation rate of battery, DEG_{BES}	0.1%
Hours of autonomy, HA	12, 24, 36, 48, 60 hrs

3.3. Diesel Generator Analytical Modeling

The power output of some RE resources is variable and therefore to ensure the continuous supply of power to the load, the

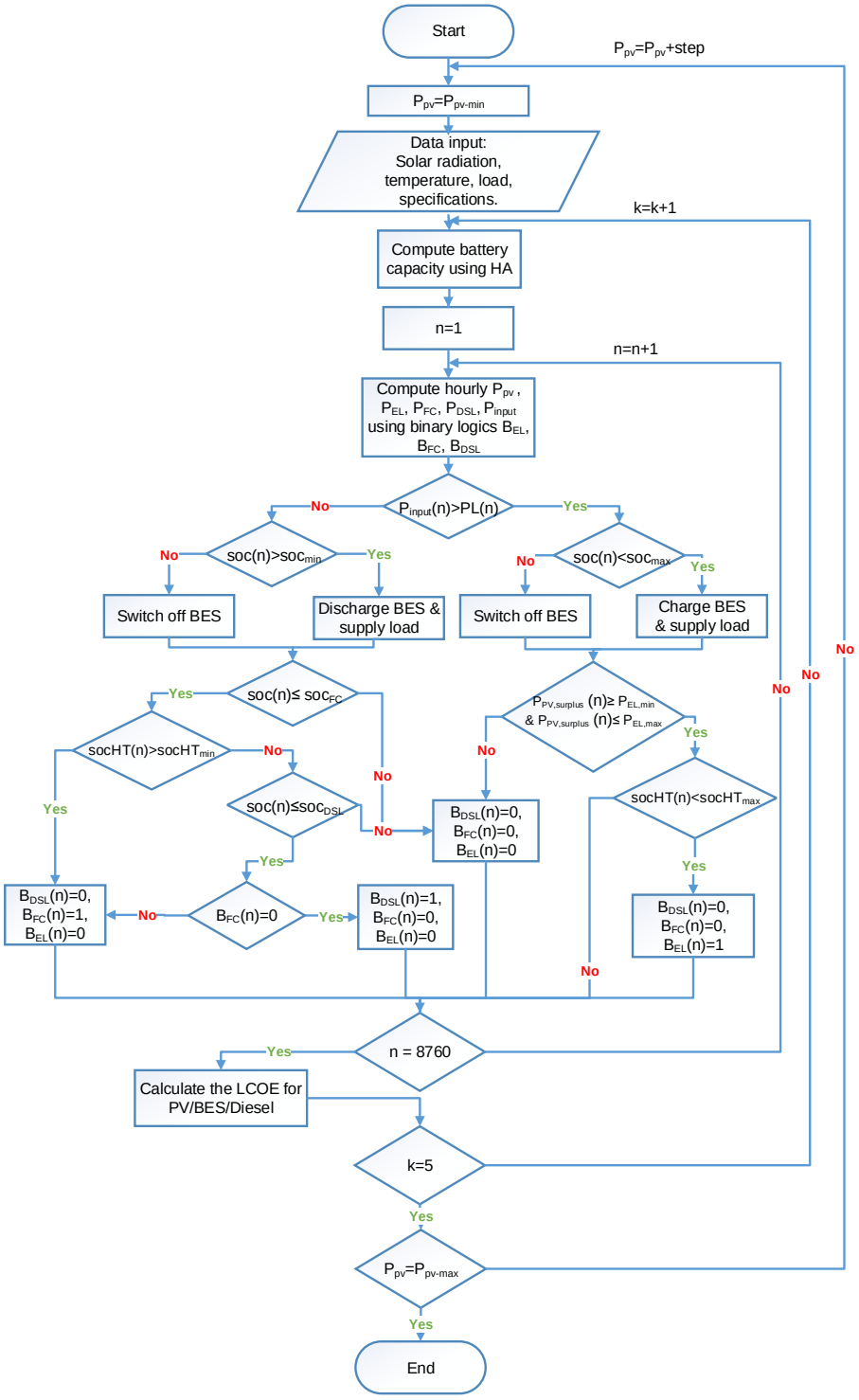

Figure 5: Flowchart that describes the analytical and economic sizing used for the intial sizing in the integrated framework.

existence of the DSL in the HES is necessary. During events, such as insufficient supply from BES and RE/AE resources, the DSL supplies the remaining load and any surplus in the DSL power will be used to charge the BES [45]. Since the first priority is to ensure load satisfaction at all times, the size of the DSL depends on PL_{max} (Fig. 7) and expressed by the following equation:

$$P_{DSL,rated} = M_{DSL} \cdot PL_{max} \quad , \tag{11}$$

M_{DSL} is the DSL margin coefficient for safety purposes, and in our study, we assumed M_{DSL} is 1.2. According to this equation, $P_{DSL,rated}$=32 kW. The hourly output of DSL is illustrated in

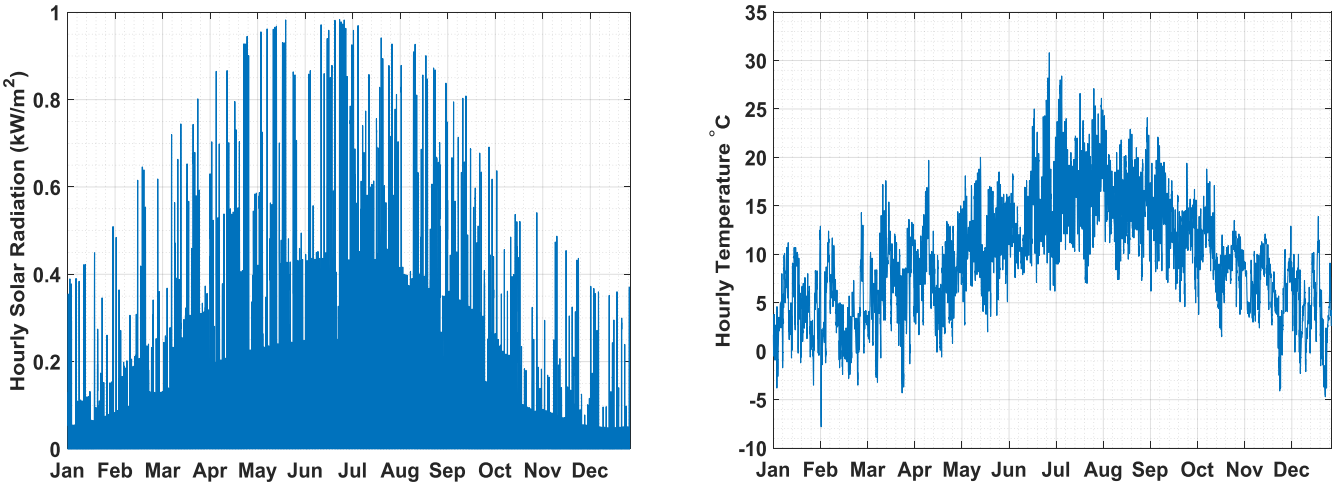

(a) (b)

Figure 6: Input data to the system for one year for Newcastle city [43]: (a) hourly solar radiation profile; (b) hourly ambient temperature profile.

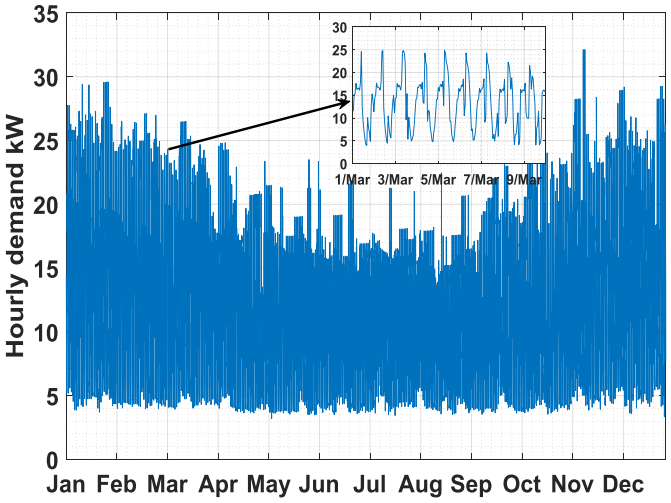

Figure 7: Demand profile for Newcastle city for one year [41].

Eq. (12) and subject to the constraint in Eq. (13) :

$$P_{DSL}(n) = \begin{cases} B_{DSL}(n) \cdot PL(n), & B_{DSL}(n) = 1\ , \\ 0, & B_{DSL}(n) = 0\ , \end{cases} \tag{12}$$

$$0 \le P_{DSL}(n) \le P_{DSL,rated}\ , \tag{13}$$

where $B_{DSL}(n)$ is a binary variable that describes the state of the DSL at a specific hour in the year [46, 47] and determined hourly to decide whether to activate the DSL or not. Condition 14 in Table 1 illustrates the constraints on DSL operation.

3.4. Fuel Cell Analytical Modeling

A FC is used as a backup power generator. The FC needs to be activated when the solar energy is insufficient to supply the demand, and depending on the battery state of charge. Any surplus in the FC power will be used to charge the BES. The size of the FC is determined using the following equation:

$$P_{FC,rated} = M_{FC} \cdot PL_{max}\quad , \tag{14}$$

where the FC margin coefficient M_{FC} is equal to 20% higher than the maximum load to leave some safe margin [48]. According to this equation, $P_{FC,rated}$= 32 kW. The hourly output power from the FC can be identified by Eq. (15) and its constraint by Eq. (16):

$$P_{FC}(n) = \begin{cases} B_{FC}(n) \cdot PL(n), & B_{FC}(n) = 1\ , \\ 0, & B_{FC}(n) = 0\ , \end{cases} \tag{15}$$

$$0 \le P_{FC}(n) \le P_{FC,rated}\quad , \tag{16}$$

$B_{FC}(n)$ is a binary variable that describes the state of the FC at any hour in the year [46, 47]. Condition 20 in Table 1 shows the constraint on FC operation. The input hydrogen to the FC is consumed from the HT. The consumption of hydrogen of rated power 1 kW in one hour can be calculated by [17]:

$$\begin{aligned} H_{2,cons,1kW} &= \frac{1kW}{2 \cdot V_{FC} \cdot F} \cdot 3600 \\ &= \frac{1000}{2 \cdot 0.7 \cdot 96487} \cdot 3600 = 26.8\ mol/h\quad , \end{aligned} \tag{17}$$

where $H_{2,cons,1kW}$ the amount of hydrogen consumed by the FC at 1 kW and depends on the FC voltage V_{FC}, and Faraday constant F (see Table 4). Based on Eq. (17), by multiplying the value of $H_{2,cons,1kW}$ by the hourly output power of the FC $P_{FC,t}$, the hourly amount of hydrogen consumed by the FC $H_{2,cons}(n)$ can be found using Eq. (18).

$$H_{2,cons}(n) = \begin{cases} P_{FC}(n) \cdot H_{2,cons,1kW}, & P_{FC}(n) > 0\ . \\ 0, & P_{FC}(n) \le 0\ . \end{cases} \tag{18}$$

3.5. Electrolyzer Analytical Modeling

The function of the EL is to produce hydrogen through the electrolysis of water [49]. The produced hydrogen is stored in a HT and used as needed to operate a FC. The output pressure of hydrogen is considered 20 bar in this paper [50]. The hourly

input power to the EL and its constraints can be identified by Eq. (19) and Eq. (20):

$$P_{EL}(n) = \begin{cases} B_{EL}(n) \cdot P_{PV,surplus}(n), & B_{EL}(n) = 1\ , \\ 0, & B_{EL}(n) = 0\ , \end{cases} \quad (19)$$

$$P_{EL,min} \leq P_{EL}(n) \leq P_{EL,rated}\ , \quad (20)$$

where $P_{EL,rated}$ is the EL rated power, $P_{EL,min}$ is the EL minimum power and equals to $20\% \cdot P_{EL,rated}$. $B_{EL}(n)$ represents a binary variable that describes the state of the EL at any hour in the year [46, 47]. The value of $B_{EL}(n)$ is determined hourly to decide whether to operate the EL or not. Condition 17 in Table 1 defines the EL operation.

If the value of the PV surplus power $P_{PV,surplus}$(n) is sufficient to operate the EL and the state of charge of HT is less than the maximum, $B_{EL}(n)$ will be set to one and the EL will generate hydrogen. To start up the EL to generate hydrogen, the value of the working voltage between its electrodes V_{el} needs to be 2 *volts* [17]. According to Faraday's law, the amount of hydrogen produced by rated power 1 kW EL in 1 h, $H_{2,prod,1kW}$, can be calculated by [17]:

$$\begin{aligned} H_{2,prod,1kW} &= \frac{1kW}{2 \cdot V_{el} \cdot F} \cdot 3600 \\ &= \frac{1000}{2 \cdot 2 \cdot 96487} \cdot 3600 = 9.33\ mol/h \quad . \end{aligned} \quad (21)$$

All the values used in calculations can be found in Table 4. Based on Eq. (21), by multiplying the value of $H_{2,prod,1kW}$ by the hourly input power to the EL $P_{EL}(n)$, the hourly amount of hydrogen produced by the EL, $H_{2,prod}(n)$, can be determined as in Eq. (22).

$$H_{2,prod}(n) = \begin{cases} P_{EL}(n) \cdot H_{2,prod,1KW}, & P_{EL}(n) > 0\ . \\ 0, & P_{EL}(n) \leq 0\ . \end{cases} \quad (22)$$

$P_{EL,rated}$ is chosen to be 100 kW in this study.

3.6. Hydrogen Tank Analytical Modeling

A HT is required to store the hydrogen produced by the EL for later use by the FC [49]. This model assumes that during the process of adding hydrogen to the tank, no energy is used and the tank experiences no leakage. Hydrogen energy produced by the EL provides another option for storing surplus PV energy.

The size of the HT S_{HT} in kgs is determined by Eq. (23), while E_{HT} is tank size in kWh given by Eq. (24) [17]:

$$S_{HT} = HA_{H_2} \cdot H_{2,prod,1kW} \cdot P_{rated,EL} \cdot H_2mass \quad , \quad (23)$$

$$E_{HT} = HA_{H_2} \cdot H_{2,prod,1kW} \cdot P_{rated,EL} \cdot H_2mass \cdot LHV \quad , \quad (24)$$

HA_{H2} is the hours of autonomy for HT and considered 48 hours in this study, H_2mass is the molar mass of hydrogen gas, and LHV is hydrogen low heating value, see Table 4. According to Eq. (23) and Eq. (24), the size of HT is 89.5 kg and 2955 kWh.

The level of hydrogen in the tank increases if the EL is operating while it decreases when the FC is producing power. Eq. (25) determines the hourly state of charge of the HT $socHT(n)$ in both cases.

Table 4: Data used for hydrogen system analytical modeling.

Parameter	Value	Ref.
$socHT_{min}$	10%	
$socHT_{max}$	90%	
Pressure, P_{HT}	20 bar	[50]
Faraday constant, F	96487 C/mol	[17]
Fuel cell voltage, V_{FC}	0.7 volts	[17]
Electrolyzer voltage, V_{el}	2 volts	[17]
H_2 low heating value, LHV	33 kWh/kg	[17]
Mole mass of H_2 gas, H_2mass	0.002 kg/mol	[17]
Fuel cell margin coefficient, M_{FC}	1.2	[48]
H_2 tank hours of autonomy, HA_{H_2}	48 hrs	

$$socHT(n) = \begin{cases} socHT(n-1) + \dfrac{H_{2,prod}(n) \cdot H_2mass \cdot LHV}{E_{HT}}, & P_{EL}(n) > 0, \\ socHT(n-1) - \dfrac{H_{2,cons}(n) \cdot H_2mass \cdot LHV}{E_{HT}}, & P_{FC}(n) > 0, \end{cases} \quad (25)$$

where $socHT(n-1)$ is the hydrogen level in the tank at time $n-1$, at any time the $socHT(n)$ is subjected to the following constraint:

$$socHT_{min} \leq socHT(n) \leq socHT_{max} \quad (26)$$

3.7. Economical Modeling

LCOE methods are widely used to evaluate the economic feasibility of RE sources. The costs distributed over the project lifetime are considered and this provides more accurate economic picture of the project under analysis [40]. In general, the LCOE is the total system cost across its lifetime divided by the energy generated from that system also across the lifetime. Eq. (27) represents the form of LCOE.

$$\begin{aligned} LCOE &= \frac{Total\ System\ Costs}{Total\ Energy\ Production}\ (£/kWh) \\ &= \sum_{j=0}^{N} \frac{\frac{Cost_{system}}{(1+r)^j}}{\frac{E_{system}}{(1+r)^j}} \quad , \end{aligned} \quad (27)$$

the total system cost $Cost_{system}$ is the sum of the total costs of the PV, BES, DSL and the inverters in the HES (as mentioned in Section 3) as presented in Eq. (28).

$$Cost_{system} = C_{PV} + C_{BES} + C_{DSL} + C_{Inv} \quad . \quad (28)$$

where C_{PV} is the total cost of PV, C_{BES} is the total cost of BES, C_{DSL} is the total cost of the DSL, and C_{Inv} is the cost of the inverters for the PV and BES. The total cost for any system can be written as in Eq. (29)

$$C_{system} = IC_{system} + OM_{system} + RC_{system} \quad . \quad (29)$$

Table 5: Hybrid energy system components' costs and lifetime used for LCOE calculation [40, 51].

Component	IC	Yearly OM	RC	Lifetime
PV	2508 £/kW	33 £/kW	0	20 years
Diesel	374 £/kW	0.1 £/kW	356 £/kW	15,000 hrs
Inverter	560 £/kW	5.6 £/kW	560 £/kW	10 years
Battery	700 £/kWh	14 £/kWh	700 £/kWh	10 years

where C_{system} is the cost of the HES in £, IC_{system} is the initial cost of all the assets in the HES, OM_{system} is the operation and maintenance cost of all the assets and RC_{system} is the replacement costs of the assets that need to be replaced.

$$E_{system} = E_{PV,T} + E_{BES,T} + E_{DSL,T} \quad , \tag{30}$$

where E_{system} represents the total energy generated by the PV/BES/diesel.

3.7.1. PV Economic Modeling

The total cost of PV is the sum of the initial costs. maintenance costs and replacement costs. The lifetime for PV is 20 years which the same as the project lifetime, so there are no replacement costs. Eq. (31) illustrates the total costs for PV.

$$C_{PV} = IC_{PV} + \frac{\sum_{j=0}^{j=N} C_{PV,OM}}{(1+r)^j} \quad , \tag{31}$$

where N is the project lifetime which is 20 years, r is the discount rate and considered to be 5%. The total energy generated from the PV discounted during its lifetime $E_{PV,T}$, can be found using the following equation:

$$E_{PV,T} = \sum_{j=0}^{j=N} \frac{\sum_{n=0}^{n=8760} E_{PV} \cdot (1 - DEG_{PV})^j}{(1+r)^j} \quad , \tag{32}$$

DEG_{PV} is the degradation rate of PV and equal to 0.5%. All the costs related to PV can be found in Table 5.

3.7.2. Battery Energy System Economic Modeling

The BES is replaced once during the project lifetime, and its replacement cost is equal to the initial cost. The total cost of the BES is calculated using the following equation:

$$C_{BES} = IC_{BES} + \frac{\sum_{j=0}^{j=N} C_{BES,OM}}{(1+r)^j} + \frac{\sum_{j=10} RC_{BES}}{(1+r)^j} \quad , \tag{33}$$

The energy produced by the BES can be found using Eq. (34).

$$E_{BES,T} = \eta_{rt} \cdot \sum_{j=0}^{j=N} \frac{\sum_{n=0}^{n=8760} E_{PV,charge} \cdot (1 - DEG_{BES})^j}{(1+r)^j} \quad , \tag{34}$$

where $E_{PV,charge}$ is the PV energy used to charge the BES, η_{rt} is the round trip efficiency for the BES and DEG_{BES} is the degradation rate for the BES.

Table 6: Data used for PV, BES, and diesel generator used economic models calculations.

Parameter	Value	Ref.
Project lifetime, N	20 years	
Discount rate, r	5%	[40]
Fuel unit cost, f_p	1.2 £/L	[54]
Round trip efficiency, η_{rt}	90%	[40]
PV degradation rate, DEG_{PV}	0.5%	[40]
BES degradation rate, DEG_{BES}	0.1%	[40]
Fuel curve intercept coefficient, A	0.246 L/kWh	[52, 53]
Fuel curve slope, B	0.08145 L/kWh	[52, 53]

3.7.3. Diesel Generator Economic Modeling

The total cost of DSL includes also the cost of fuel, Eq. (35) and Eq. (36) show the fuel consumed by the DSL and its cost respectively [52].

$$F_{consume}(n) = \begin{cases} A \cdot P_{DSL,rated} + B \cdot P_{DSL}(n), & P_{DSL}(n) > 0. \\ 0, & P_{DSL}(n) = 0. \end{cases} \tag{35}$$

$$C_{DSL,fuel}(n) = \begin{cases} F_{consume}(n) \cdot f_p, & F_{consume}(n) > 0. \\ 0, & F_{consume}(n) = 0. \end{cases} \tag{36}$$

where A and B are the coefficients of the fuel consumption curve, 0.246 and 0.08145 respectively [52, 53]. The DSL lifetime is given in hours, $Life_{DSL,h}$, and can be found in years using Eq. (37), $Life_{DSL,y}$ is necessary to calculate the replacement cost for the DSL.

$$Life_{DSL,y} = \frac{Life_{DSL,h}}{WH_{DSL}} \quad . \tag{37}$$

The total cost of the DSL can be found using the following equation:

$$\begin{aligned} C_{DSL} = & IC_{DSL} + \frac{\sum_{j=0}^{j=N} C_{DSL,OM}}{(1+r)^j} + \\ & \frac{\sum_{j=Life_{DSL,y}} RC_{DSL}}{(1+r)^j} + \frac{\sum_{j=0}^{j=N} C_{DSL,fuel}}{(1+r)^j} \quad , \end{aligned} \tag{38}$$

and the energy generated by the DSL is calculated using Eq. (39).

$$E_{DSL,T} = \sum_{j=0}^{j=N} \frac{\sum_{n=0}^{n=8760} E_{DSL}}{(1+r)^j} \quad . \tag{39}$$

3.8. Reliability Analysis

Reliability is a key performance indicator in sizing and operation of a power system [55, 56]. The eliability index used in this study is loss of power supply probability (LPSP). LPSP is an indecator used to measure how an energy system is capable to supply enough power to the load during a certain period. It is defined as the ratio of energy deficiency to load during a certain period. The lower LPSP the more reliable operation of the power system, where if LPSP equals zero means the istalled

RE/AE resources can cover the load is continously supplied. Whereas if LSPS is one indicates that the load is never fed [57]. The below equation illustates how LPSP can be computed.

$$LPSP = \frac{\sum_{n=1}^{8760} DE(n)}{\sum_{n=1}^{8760} PL(n)} \quad , \tag{40}$$

where $DE(n)$ and $PL(n)$ represent the deficiency in energy and the demand during a certain time respectively.

3.9. Objective Function and Constraints

The objective function of the optimum design problem is the minimization of the LCOE of the PV/BES/DSL while satisfying the operational constraints. PV rated power, BES hours of autonomy and fuel cost are the state variables of the optimization study. When these values were optimized, the objective function was expected to get the lowest value. The objective function is defined by Eq. (41).

$$min\ LCOE = min \sum_{j=0}^{N} \frac{\frac{Cost_{system}}{(1+r)^j}}{\frac{E_{system}}{(1+r)^j}} \quad , \tag{41}$$

where $Cost_{system}$ is expressed by Eq. (28), and E_{system} is expressed by Eq. (30).

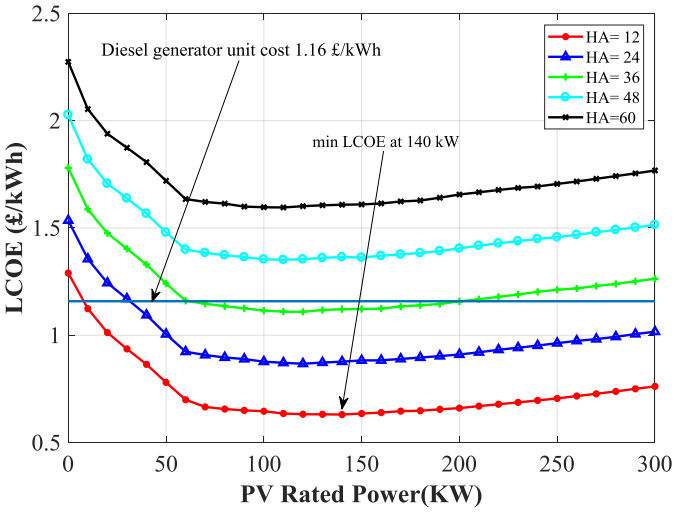

Figure 8: Levelized cost of energy for the HES when using AES approach and for five values of HA.

Table 7: The size of HES based on $EMS_{initial}$ based on AES approach.

Subsystem	Size
PV / inverter	140 kW / 154 kW
Battery energy system / inverter	218 kWh / 29.4 kW
Diesel generator	32 kW
Electrolyzer / inverter	100 kW / 110 kW
Fuel cell / inverter	32 kW / 35.2 kW
Hydrogen Tank	89.5 kg

Table 8: Operating conditions used for EMS_1 operation.

Condition	Description
10-14	same as in Table 1
15	$soc(n) > soc_{DSL}$
16	$P_{input} > PL$
17	$P_{PV,surplus}(n) > 0$ & $socHT(n) < socHT_{max}$
18	$socHT(n) \geq socHT_{max}$
19	$P_{input}(n) < PL(n)$ & $Jan < n < Jun$ & $soc(n) \leq soc_{FC}$ & $socHT(n) > socHT_{min}$
20	$P_{input}(n) < PL(n)$ & $Oct < n < Dec$ & $soc(n) \leq soc_{FC}$ & $socHT(n) > socHT_{min}$
21	$socHT(n) \leq socHT_{min}$

For a hybrid PV/BES/diesel system, the following operational constraints should be satisfied. All these constraints have been explained in Section 3.

$$0 \leq P_{PV,rated} \leq \alpha PL_{max} \quad , \tag{42}$$

$$12 < HA < 60 \quad , \tag{43}$$

$$0 \leq P_{DSL}(n) \leq P_{DSL,rated} \quad , \tag{44}$$

3.10. Initial Sizing

The AES approach has been discussed thoroughly in Section 3. AES is the first step in the integrated framework as illustrated in Fig. 9. The output of this step is the initial size of the HES using $EMS_{initial}$. Fig. 8 presents the output results of the AES approach. Each colored line represents the LCOE values for a specific BES HA and over the $P_{PV,rated}$ range from 0 to 267 kW. The results are compared to the cost of a DSL assuming that this DSL is the only source for supplying the load, and represented by the blue straight line. Such unitary energy cost, corresponding to the LCOE with no RE/AE sources integrated, is calculated in Eq. (45) [42].

$$U_{DSL} = \frac{SFC \cdot f_p}{EL_{total}} \quad , \tag{45}$$

where f_p is the fuel cost, EL_{total} is the total energy of the load for one year, SFC is the specific fuel consumption for DSL and calculated using the following equation:

$$SFC = A \cdot PL_{max} \cdot n + B \cdot EL_{total} \quad . \tag{46}$$

where n is the number of hours in one year, A and B are the DSL consumption curve coefficients, and PL_{max} is the maximum load.

Our objective in the first step of the framework is to optimize the size of PV/BES/DSL and ensure achieving the minimum LCOE at the same time. According to Fig. 8 the minimum LCOE is obtained when $P_{PV,rated}$ is equal to 140 kW, and 12 hours of autonomy for the BES. The BES capacity at 12 hours of HA is 218 kWh using Eq. (7). The obtained HES components' sizes are presented in Table 7.

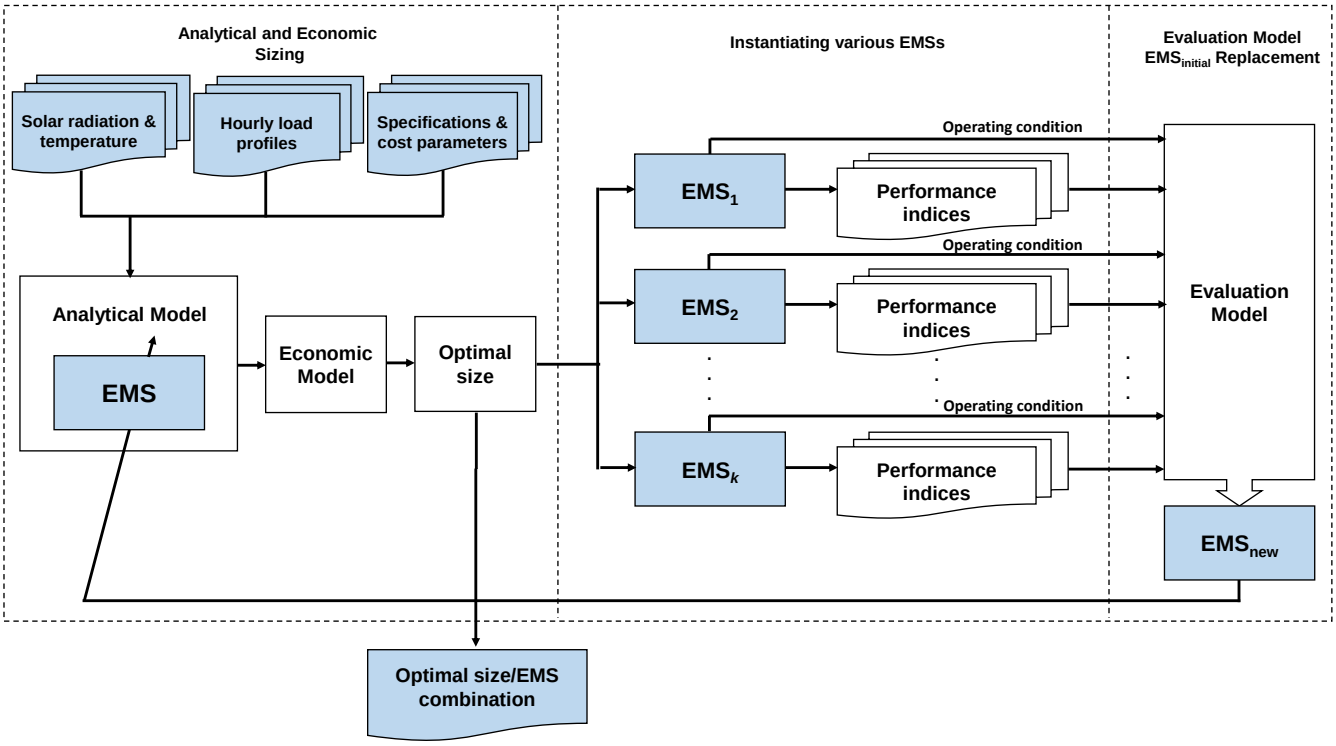

Figure 9: Stylized demonstration of three-step proposed framework: (1) analytical and economic sizing; (2) using FA to generate various EMS; and 3) evaluation model and replacing $EMS_{initial}$.

4. Integrated Framework

Figure 9 illustrates the proposed integrated framework for finding the optimal size-EMS combination of a HES. The framework consists of three steps. The first step is applying AES approach (Section 3) to find the initial sizes of HES components based on $EMS_{initial}$. Once the sizes are obtained, they will be exercised by three different EMSs generated from $EMS_{initial}$ using FA and this is the second step. Also, a number of performance indices will be calculated for each EMS in the second step to be used by the next step. In the third step, an evaluation model is proposed to compare the performance indices of each EMS and track the conditions related to each performance index. Then the elected conditions are used to obtain EMS_{new} which will replace $EMS_{initial}$ in the first step. Finally, the optimal size-EMS combination will be achieved based on EMS_{new}. Next sections describe the integrated framework second and third steps in detail.

4.1. Instantiate Various EMSs using Finite Automata

FA is utilized to implement $EMS_{initial}$ and instantiate three EMSs such that all the EMSs have the same outline as the $EMS_{initial}$. Employing FA to implement $EMS_{initial}$ has been described in detail in Section 2.3. The instantiation process is done by generating three models of $EMS_{initial}$. Then by changing some of the operating conditions that are related to the activation of the DSL, FC, and EL, three different EMSs with different operation will be generated. The initial sizes obtained in Section 3.10 are applied using these EMSs and assessment between them are described by the performance indices, as explained in the next section.

Figures 10-12 describes the EMSs instantiated from $EMS_{initial}$ by FA and graphically represented using TCT software [34]. Below is a description of these EMSs and the changes in the operating condition with reference to $EMS_{initial}$ described in Fig. 4.

All the EMSs have the same states as in $EMS_{initial}$ and presented in Fig. 3. Figure 10 represents EMS_1 modeled in FA and the conditions are illustrated in Table 8. Conditions from 10 to 15 are the same as in $EMS_{initial}$, conditions from 10 to 13 related to the EL, while 14 and 15 controls the DSL operation. The DSL in EMS_1 when operates will provide its rated power, and any extra energy after satisfying the load will be used to charge the BES. There are changes in EL operation, the EL will exploit any surplus PV power to produce hydrogen. Where condition 16 is for switching on EL and 17 or 18 to switch it off. The FC is set to operate during a specified period in the year, from January to June and from October to December and its output power is equal to the load at the time of operation and represented by condition 19 and 20. The occurrence of conditions 21 or 22 lead to switch off the FC.

The next instantiated EMS is EMS_2 and Fig. 11 describes its FA model. The conditions are given in Table 9. Conditions from 10 to 13 (BES operation) are the same as $EMS_{initial}$ in Table 1. The condition that describes the DSL operation is either 14 or 15. Condition 14 characterizes switching on the DSL with hysteresis zone to minimize the frequency of switching. Condition 15 operates the DSL such that the generated output power

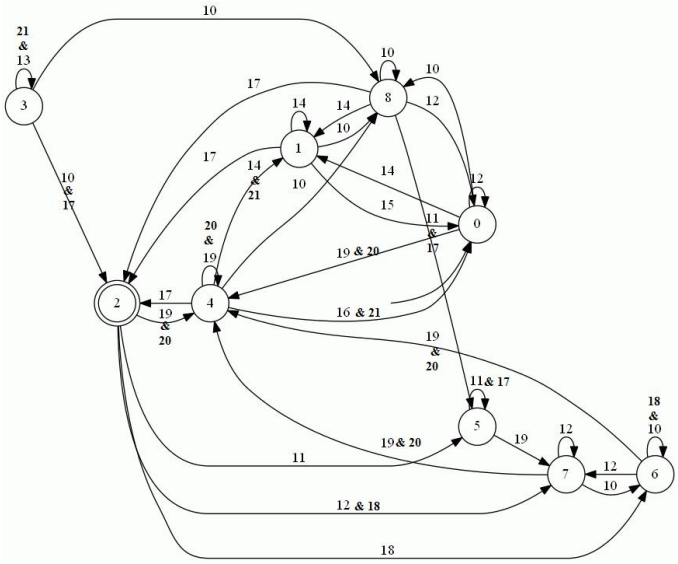

Figure 10: Implementing EMS_1 in FA and using the states described in Fig. 3.

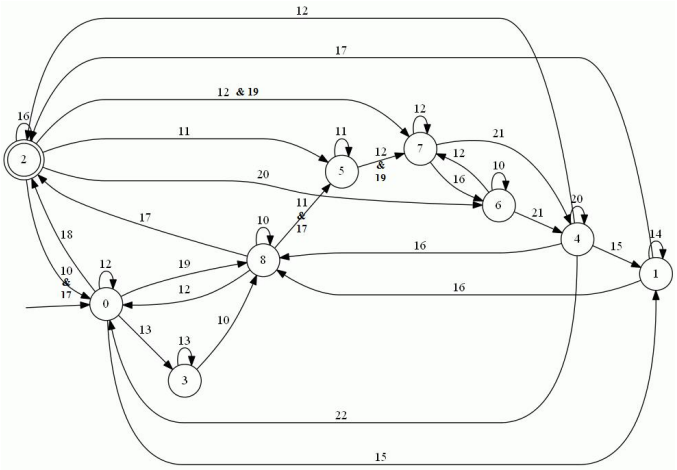

Figure 11: Implementing EMS_2 in FA and using the states described in Fig. 3.

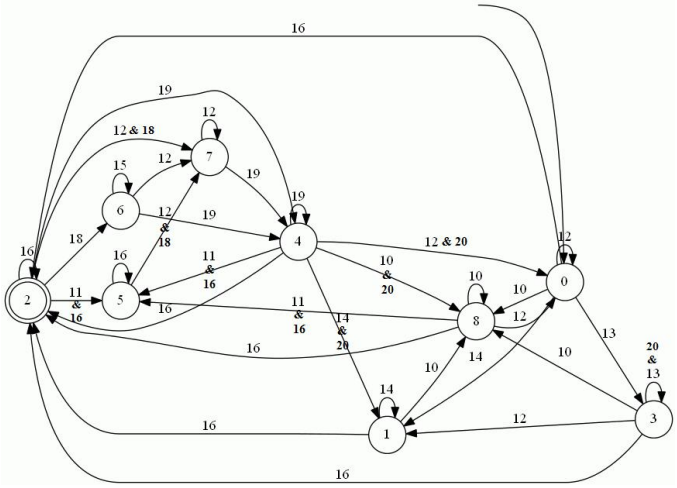

Figure 12: Implementing EMS_3 in FA and using the states described in Fig. 3.

is equal to 30% of $P_{DSL,rated}$ when $PL(n) \leq 30\% \cdot P_{DSL,rated}$, otherwise $P_{DSL}(n) = PL(n)$. Condition 16 is for switching off the DSL. The FC operation is also controlled by hysteresis zones as in condition 20, and condition 21 is for normal operation of the FC and its output power is equal to the load. The occurrence of condition 22 will turn off the FC. Figure 12 illustrates the third instantiated EMS using FA The difference between EMS_3 and $EMS_{initial}$ is the status of BES in state 1 changed from idle to charge. The reason for this is the value of the output power from the DSL and FC are their rated power at each time they are activated. Therefore, after supplying the load, any extra power is used to charge BES. The operating conditions for EMS_3 is the same as in Table 1 with a change in the EL operating condition 16 and 17 as following:

- Condition 16 in EMS_3: $0 < P_{PV,surplus}(n) < P_{EL,min}$ & $socHT(n) < socHT_{max}$ & $soc(n) > soc_{min}$
- Condition 17 in EMS_3: $P_{PV,surplus}(n) = 0$

The EL in EMS_3 will operate if there there is any surplus PV energy even if it is less than the minimum, the EL will take energy from the BES until the energy reaches its minimum rated power. But before that the BES should has enough energy to supply the EL.

The three instantiated EMSs along with $EMS_{initial}$ are simulated with the initial sizes and a number of performance indices are computed. These indices are the input to the third step in the integrated framework, the evaluation model and $EMS_{initial}$ replacement.

4.2. Performance Indices

There are multiple performance indices have been adopted to asses the instantiated EMSs. Working hours for the DSL, FC and EL WH_{DSL}, WH_{FC} and WH_{EL} respectively are among these indices. Table 11 shows the performance indices used in the evaluation model. Along with the working hours of the above-mentioned components, the LCOE, fuel cost, PV contribution, and system overall efficiency are also selected for the evaluation. WH_{DSL} is an important index since one of the desired properties in the optimal EMS is to reduce the working

Table 9: Operating conditions used for EMS_2 operation.

Conditions	Description
10-13	same as in Table 1
14	$P_{input}(n) < PL(n)$ & $soc_{DSL} < soc(n) < 30\%$ & $B_{DSL}(n-1) = 1$ & $B_{FC}(n) = 0$
15	$P_{input}(n) < PL(n)$ & $soc(n) \leq soc_{DSL}$ & $B_{FC}(n) = 0$
16	$P_{input}(n) > PL(n)$
17	$P_{EL,min} \leq P_{PV,surplus}(n) \leq P_{EL,rated}$ & $socHT(n) < socHT_{max}$
18	$P_{PV,surplus}(n) < P_{EL,min}$
19	$socHT(n) \geq socHT_{max}$
20	$soc_{FC} \leq soc(n) \leq 40\%$ & $socHT(n) > socHT_{min}$ & $B_{FC}(n-1) = 1$
21	$soc(n) \leq soc_{FC}$ & $socHT(n) > socHT_{min}$
22	$socHT(n) \leq socHT_{min}$

hours of the DSL as well as the fuel cost. Moreover, the objective function of this study (Section 3.9) is to minimize the LCOE, so comparing the LCOE for the four EMSs will give an indication if the generated EMS_{new} satisfies this objective or not. PV contribution also an important index that represents the percentage of utilized PV energy in BES charging, supplying the load and activating the EL. Finding this index can help in obtaining an EMS that exploits higher PV energy and reduces PV energy losses.

4.3. Evaluation Model and $EMS_{initial}$ Replacement

To carry out the analysis, an evaluation model is introduced to compare all the output performance indices in Table 11 for all the instantiated EMSs and $EMS_{initial}$ as well. The purpose of the evaluation model is to select the operating conditions that lead to the most reliable performance of the HES. After determining the most reliable indices for each EMS, the function of the evaluation model is to track the operating conditions related to each reliable index and employ these operating conditions in the new EMS. the following gives an illustration regarding the evaluation process:

- It is observed from Table 11 that WH_{DSL} is minimum for EMS_1, because the DSL operated at its rated power. So the condition that controls the operation of the DSL in EMS_1 is adopted to be used in EMS_{new}.
- It is better also to minimize WH_{FC} because of the high cost of the FC operation. By looking at Table 11, it is noticed that WH_{FC} is minimum for EMS_3. Therefore, this condition is elected to be in EMS_{new}.
- WH_{EL} is maximum for EMS_3, higher WH_{EL} means more H_2 generation. Similarly, the condition of the EL in EMS_3 is chosen to be used in EMS_{new}.
- The LCOE and fuel cost calculated for all the EMSs are minimum for EMS_1, this because the WH_{DSL} is minimum and this leads to minimization of fuel cost.
- The PV contribution for EMS_3 is the highest, this explains the highest WH_{EL}.
- It is clear that the η_{sys} for all the EMSs is almost the same, which means η_{sys} has no effect on choosing the operating conditions but will be used later for comparison between AES sizing and the integrated framework.

The values of $EMS_{initial}$ and EMS_2 performance indices in Table 11 are always mediate between EMS_1 and EMS_3, therefore none of the operating conditions of these EMSs are used in EMS_{new} generation. To this end the EMS_{new} is generated by the evaluation model and its FA representation is described by Fig. 13 and the featured operating conditions can be found in Table 10.

According to Table 11, it is clear that the performance indices for EMS_{new} have better values when compared to all the indices of the EMSs in terms of WH_{DSL}, WH_{FC}, LCOE, fuel cost and PV utilization.

Thus, the $EMS_{initial}$ will be replaced by EMS_{new}. Following that, the AES approach can be re-exercised to generate an enhanced size of the HES based on EMS_{new}. The results of the integrated framework are discussed in the following section.

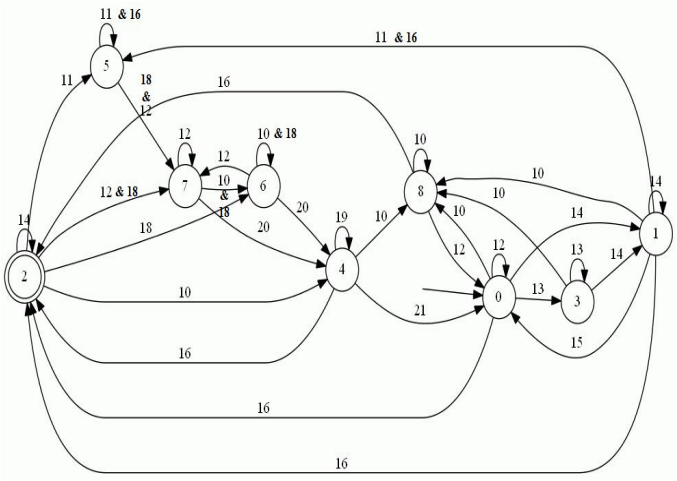

Figure 13: Implementing EMS_{new} in FA and using the states described in Fig. 3.

Table 10: Operating conditions used for EMS_{new} operation.

Conditions	Description
10	$P_{input}(n) \geq PL(n)$ & $soc(n) < soc_{max}$
11	$soc(n) \geq soc_{max}$
12	$P_{input}(n) < PL(n)$ & $soc(n) > soc_{DSL}$
13	$soc(n) \leq soc_{min}$
14	$P_{input}(n) < PL(n)$ & $soc(n) \leq soc_{DSL}$ & $B_{FC} = 0$
15	$P_{input}(n) > PL(n)$
16	$0 < P_{PV,surplus}(n) < P_{EL,min}$ & $socHT(n) < socHT_{max}$ & $soc(n) > soc_{min}$
17	$P_{PV,surplus}(n) = 0$
18	$socHT(n) \geq socHT_{max}$
19	$P_{input}(n) < PL(n)$ & $soc_{FC} < soc(n) \leq 40\%$ & $socHT(n) > socHT_{min}$ & $B_{FC}(n-1) = 1$
20	$P_{input}(n) < PL(n)$ & $soc(n) \leq soc_{FC}$ & $socHT(n) > socHT_{min}$
21	$soc(n) > soc_{FC}$
22	$socHT(n) \leq socHT_{min}$

5. Results and Discussion

The simulations were done using real data profiles for both PV and load (Fig. 6). Firstly, a PV/Diesel/BES/Hydrogen sys-

Table 11: Performance indices that used asses the instantiated EMSs.

Index	$EMS_{initial}$	EMS_1	EMS_2	EMS_3	EMS_{new}
$WH_{DSL}(hrs)$	1994	800	1975	2276	793
$WH_{FC}(hrs)$	525	487	470	136	162
$WH_{EL}(hrs)$	224	322	213	337	396
$LCOE$(£/kWh)	0.6306	0.4337	0.5846	0.6041	0.4141
Fuel cost (£)	21,037	10,061	21,197	24,030	9,973.2
PV contribution	57%	57%	57%	59%	57%
η_{sys}	89%	88%	88%	88%	89%

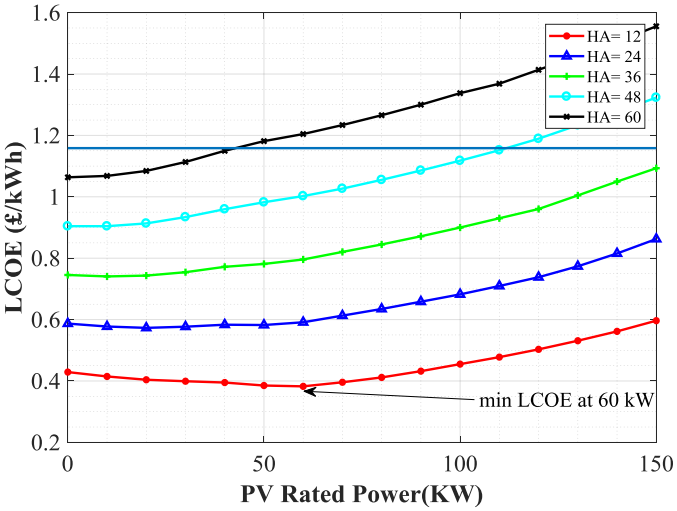

Figure 14: Levelized cost of energy for the HES when using the integrated framework.

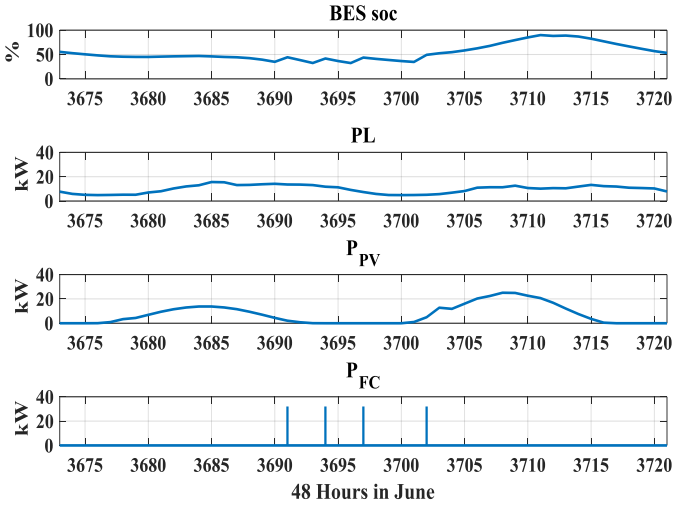

Figure 15: Battery soc, load, FC and PV power values during 48 hours in June, the DSL output is zero during these hours.

tem HES having an initial EMS is examined using AES approach and the results are analyzed. Then, the same HES is examined using the proposed integrated framework, and the obtained sizing results are then compared to the results of the initial sizing.

Table 7 and Table 12 show the sizing results of HES components using AES approach and integrated framework respectively. Notice that the PV is the main component in the HES in terms of installed capacity in both cases. The BES, DSL and FC remained the same sizing for both approaches. The DSL and FC sizes depend only on the maximum load, so any change in the sizes of HES subsystems will not affect these two subsystems. On the other hand, the size of BES as calculated from Eq. (7) also depends on the average load and HA.

As observed in Fig. 8 and Fig. 14 the PV and BES sizes are determined based on the minimum LCOE for the PV/BES/DSL system only. For AES approach and the integrated framework, the minimum LCOE obtained when $HA = 12\ hrs$. This explains why BES remains the same capacity. $P_{PV,rated} = 140\ kW$

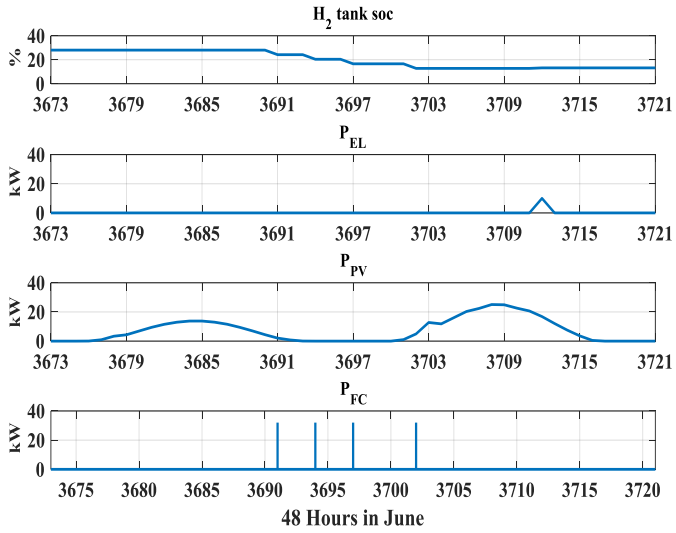

Figure 16: Hydrogen tank soc, EL, PV, FC power values during 48 hours in June.

when using AES approach and $P_{PV,rated} = 60\ kW$ when applying the integrated framework. There is a 42% increase in PV contribution (as detailed in Table 13), and therefore, a decrease in PV energy losses. $P_{EL,rated}$ in AES approach is assumed to be 100 kW (see Section 3.5). However, the LCOE and WH_{DSL} and hence the fuel cost are substantially reduced. EMS_{new} and as a result, there is a reduction in the size of some components. Accordingly, the EL rated power is found to be 50 kW. $P_{FC,rated}$ remains the same, and the HT size is based on the EL size and is calculated to be 45 kg. The new sizes for the hydrogen system are used in the resizing process of the integrated framework with the EMS_{new} to obtain new sizes for the PV/BES. The results obtained by the AES approach and the integrated framework for standalone HES are shown in Table 7 and Table 12. It is clear that using the integrated framework leads to a significantly lower size for the PV. However, even though the sizes of BES and DSL stayed the same, the performance indices related to them shown an improvement in performance. For example, as shown in Table 13, the operation hours of DSL and FC decreased by 35% and 83% respectively. Moreover, the LCOE is reduced by 40% and the fuel cost is decreased by 23%. In addition, more utilization of PV energy is obtained by using the framework as the PV contribution increased to 98%, indicating that the PV energy is almost fully exploited. Applying the integrated framework yielded also to a reduction in the replace-

Table 12: The optimal size of the HES using the integrated framework.

Subsystem	Size
PV / inverter	60 kW / 66 kW
Battery energy system / inverter	218 kWh / 29.4 kW
Electrolyzer / inverter	50 kW / 55 kW
Fuel cell / inverter	32 kW / 35.2 kW
Diesel generator	32 kW
Hydrogen Tank	45 kg

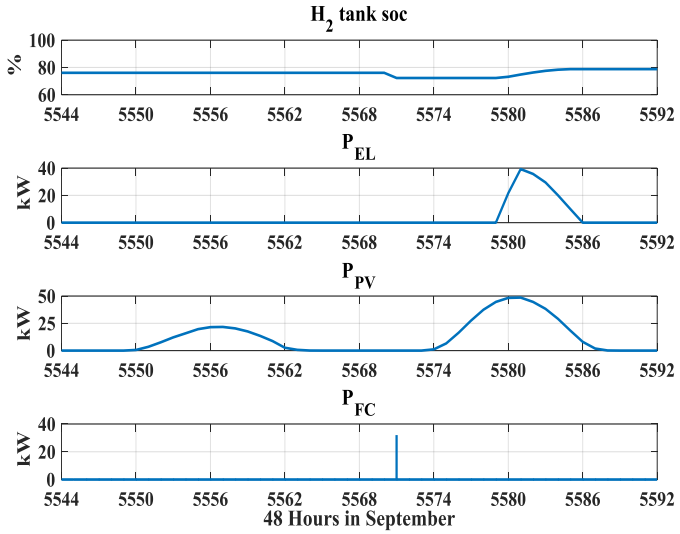

Figure 17: Hydrogen tank soc, EL, PV, and FC power values during 48 hours in September.

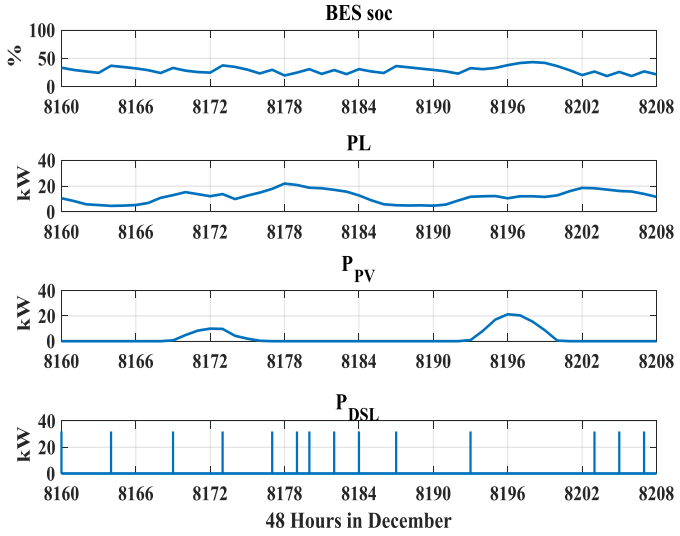

Figure 18: Battery soc, load, PV, DSL power values during 48 hours in December.

ment cost of the DSL by half, as the DSL is replaced twice during the HES lifetime compared to three times when using AES approach.

The LPSP as described in Section 3.8 indicates how the system is reliable by finding the probability that the HES is unable to supply the load. By looking at LPSP values in Table 13 it is noticed that their values are zero, this expected as at the times where there are insufficient energy from RE/AE resources or the BES, the diesel generator will supply the demand with power equivalent to its rated power. The LPSP can be recognized more in undersized systems, in this study the sizing obtained by AES is considered oversized while the size obtained by the integrated framework is the optimal sizing. Based on this the value of LPSP will be zero for AES and integrated framework.

Fig. 15 demonstrates values of *soc*, P_{Load}, P_{PV} and P_{FC} for 48 hours in June as a result of applying the integrated framework. The DSL output power is zero during that period since

Table 13: Comparison between the results obtained by using AES approach and the integrated framework.

Index	AES	Framework	Improvements
WH_{DSL} (hrs)	1994	1293	35% reduction
WH_{FC} (hrs)	525	88	83% reduction
WH_{EL} (hrs)	224	356	37% increase
$LCOE$ (£/kWh)	0.6300	0.3809	40% reduction
Fuel cost (£)	21037	16262	23% reduction
PV contribution	57%	98%	41.8% increase
$life_{DSL}$ $(years)$	8	12	50% reduction in RC_{DSL}
η_{sys}	90	93	7% increase
LPSP	0	0	0

there is available PV energy and *soc* is between 30% and 90%. The load ranges between 5-15 kW, during daylight and the BES and PV power cover the load. During night hours, BES goes below 35% and with available H_2 in the HT, the FC is activated. The FC operated four times, generating its rated power each time. Any extra power is used to charge BES. This also can be seen in Fig. 16, which represents HT levels, P_{EL} and P_{FC} power values during the same 48 hours in June. Fig. 16 shows that *socHT* starts to decrease when P_{FC} is on, and has a slight increase when P_{EL} is on due to the H_2 generation from the EL.

Since power generation, consumption, and the load are varying through the year, it is important to display them during different times in the year. Fig. 18 shows the values of BES *soc*, P_{Load}, P_{PV} and P_{DSL} for 48 hours in December as a result of applying the integrated framework. The FC output power is zero during that period as there is not enough H_2 in the tank during this time of the year. The HES depends on the DSL to satisfy the load, because the PV output during winter is low while the load is high. The DSL operated 14 times during this period generating its full rated power each time. The H_2 level is minimum during the same period, as well as the FC and EL power values are zero. In order to illustrate the hydrogen system performance when the HT is almost full, Fig. 17 represents hydrogen system values for 48 hours in September. *socHT* is 80%, the EL is operated when there is surplus PV energy while the FC is operated just once.

Finally, to ensure that the generated EMS_{new} is the optimal between all the EMSs generated by FA, simulations are carried out for EMS_1, EMS_2, EMS_3 using the new sizes of the HES to generate EMS_{1new}, EMS_{2new}, EMS_{3new}. The results in Table 14 lead to the same conclusion where the performance indices of EMS_{new} registered the minimum values in WH_{DSL},

Table 14: Performance indices for EMS_{new} and generated EMSs using the sizes from the integrated framework.

Index	EMS_{new}	EMS_{1new}	EMS_{2new}	EMS_{3new}
$WH_{DSL}(hrs)$	1293	1327	3662	3663
$WH_{FC}(hrs)$	88	37	181	85
$WH_{EL}(hrs)$	356	174	176	352
$LCOE$(£/kWh)	0.3809	0.3911	0.6688	0.6808
Fuel cost (£)	16,262	16,689	39,256	38,640
PV contribution	98%	90%	98%	98%
η_{sys}	93%	96%	96%	93%

LCOE and fuel cost.

6. Conclusion and Future Work

A novel integrated framework is successfully developed to find the optimal size-energy management strategy combination for a hybrid standalone photovoltaic/battery/diesel/hydrogen system. The novelty in this work can be summarized as taking the impact of selecting the right energy management strategy on the sizing of a hybrid energy system. This can lead to better performance and can be explained in our integrated framework by reducing the cost, reducing the diesel generator and fuel cell working hours and increasing the photovoltaic utilization. Moreover, using finite automata in implementing and instantiating multiple energy management strategies to attain an improved one has not been reported. The proposed framework consists of three consecutive steps; firstly, an analytical and economic sizing is performed using an initial energy management strategy to find the initial size of the hybrid energy system. Secondly, Finite Automata is utilized to implement the initial energy management system and instantiate various energy management strategies. A number of simulations are performed to exercise these energy management strategies using the initial sizes. A set of performance indices are also calculated for the instantiated energy management strategies in this step which will be used as entries to the next step. Following that, an evaluation model is implemented to compare the performance indices of the initial and instantiated energy management strategies. It determines the best-operating conditions to use them in generating a new EMS. The new generated EMS will replace the initial EMS, and then the analytical and economical sizing is carried out again to find the new size based on the new energy management strategy. Simulation results from the the integrated framework yield better results when compared to the results from the initial analytical and economic sizing in terms of reducing the photovoltaic, electrolyzer and hydrogen tank sizes. Moreover, the system levelized cost of electricity is reduced when using the proposed framework.

In future research work, the selection of the featured operating conditions will be done in an automatic way using the formal languages of the finite automata. This will allow the production of all possible energy management strategies from the initial energy management strategy, which will improve the whole process of generating the optimal energy management strategy. Moreover, a sensitivity analysis and uncertainty in load and photovoltaic will be added to study how will this affect the hybrid energy system sizing.

Acknowledgment

The authors would like to thank Applied Science Private University (Jordan) for their funding and support.

References

[1] L. Li, J. Sun, Y. Li, Prospective fully-coupled multi-level analytical methodology for concentrated solar power plants: General modelling, Applied Thermal Engineering 118 (2017) 171 – 187.

[2] L. Li, Y. Li, J. Sun, Prospective fully-coupled multi-level analytical methodology for concentrated solar power plants: Applications, Applied Thermal Engineering 118 (2017) 159 – 170.

[3] S. Guo, Q. Liu, J. Sun, H. Jin, A review on the utilization of hybrid renewable energy, Renewable and Sustainable Energy Reviews 91 (2018) 1121 – 1147.

[4] P. Nema, R. Nema, S. Rangnekar, A current and future state of art development of hybrid energy system using wind and pv-solar: A review, Renewable and Sustainable Energy Reviews 13 (8) (2009) 2096–2103.

[5] M. H. Nehrir, C. Wang, K. Strunz, H. Aki, R. Ramakumar, J. Bing, Z. Miao, Z. Salameh, A review of hybrid renewable/alternative energy systems for electric power generation: Configurations, control, and applications, IEEE Transactions on Sustainable Energy 2 (4) (2011) 392–403.

[6] S. Ölz, Renewable energy policy considerations for deploying renewables.

[7] A. H. Fathima, K. Palanisamy, Optimization in microgrids with hybrid energy systems – a review, Renewable and Sustainable Energy Reviews 45 (2015) 431–446.

[8] B. Madaci, R. Chenni, E. Kurt, K. E. Hemsas, Design and control of a stand-alone hybrid power system, International Journal of Hydrogen Energy 41 (29) (2016) 12485 – 12496, special Issue on 3rd European Conference on Renewable Energy Systems (ECRES 2015), 7–10 October 2015, Kemer, Antalya, Turkey.

[9] D. M. Gioutsos, K. Blok, L. van Velzen, S. Moorman, Cost-optimal electricity systems with increasing renewable energy penetration for islands across the globe, Applied Energy 226 (2018) 437 – 449.

[10] W. Zhou, C. Lou, Z. Li, L. Lu, H. Yang, Current status of research on optimum sizing of stand-alone hybrid solar–wind power generation systems, Applied Energy 87 (2) (2010) 380 – 389.

[11] A. Ehsan, Q. Yang, Optimal integration and planning of renewable distributed generation in the power distribution networks: A review of analytical techniques, Applied Energy 210 (2018) 44 – 59.

[12] M. Trifkovic, M. Sheikhzadeh, K. Nigim, P. Daoutidis, Modeling and control of a renewable hybrid energy system with hydrogen storage, IEEE Transactions on Control Systems Technology 22 (1) (2014) 169–179.

[13] J. Lagorse, D. Paire, A. Miraoui, A multi-agent system for energy management of distributed power sources, Renewable Energy 35 (1) (2010) 174 – 182.

[14] D. Giaouris, A. I. Papadopoulos, C. Patsios, S. Walker, C. Ziogou, P. Taylor, S. Voutetakis, S. Papadopoulou, P. Seferlis, A systems approach for management of microgrids considering multiple energy carriers, stochastic loads, forecasting and demand side response, Applied Energy 226 (2018) 546 – 559.

[15] D. Ipsakis, S. Voutetakis, P. Seferlis, F. Stergiopoulos, C. Elmasides, Power management strategies for a stand-alone power system using renewable energy sources and hydrogen storage, International Journal of Hydrogen Energy 34 (16) (2009) 7081 – 7095.

[16] S. Upadhyay, M. Sharma, A review on configurations, control and sizing methodologies of hybrid energy systems, Renewable and Sustainable Energy Reviews 38 (2014) 47 – 63.

[17] C. H. Li, X. J. Zhu, G. Y. Cao, S. Sui, M. R. Hu, Dynamic modeling and sizing optimization of standalone Photovoltaic power systems using hybrid energy storage technology, Renewable Energy 34 (3) (2009) 815–826.

[18] M. Smaoui, A. Abdelkafi, L. Krichen, Optimal sizing of stand-alone photovoltaic/wind/hydrogen hybrid system supplying a desalination unit, Solar Energy 120 (2015) 263 – 276.

[19] A. Maleki, A. Askarzadeh, Comparative study of artificial intelligence techniques for sizing of a hydrogen-based stand-alone photovoltaic/wind hybrid system, International Journal of Hydrogen Energy 39 (19) (2014) 9973 – 9984.

[20] M. H. Amrollahi, S. M. T. Bathaee, Techno-economic optimization of hybrid photovoltaic/wind generation together with energy storage system in a stand-alone micro-grid subjected to demand response, Applied Energy 202 (2017) 66 – 77.

[21] J. Torreglosa, P. García, L. Fernández, F. Jurado, Hierarchical energy management system for stand-alone hybrid system based on generation costs and cascade control, Energy Conversion and Management 77 (2014) 514 – 526.

[22] W.-M. Lin, C.-S. Tu, M.-T. Tsai, Energy management strategy for microgrids by using enhanced bee colony optimization, Energies 9 (1) (2016)

5.

[23] A. C. Luna, N. L. Diaz, M. Graells, J. C. Vasquez, J. M. Guerrero, Mixed-integer-linear-programming-based energy management system for hybrid pv-wind-battery microgrids: Modeling, design, and experimental verification, IEEE Transactions on Power Electronics 32 (4) (2017) 2769–2783.

[24] B. Zhao, X. Zhang, P. Li, K. Wang, M. Xue, C. Wang, Optimal sizing, operating strategy and operational experience of a stand-alone microgrid on dongfushan island, Applied Energy 113 (2014) 1656 – 1666.

[25] M. Castañeda, A. Cano, F. Jurado, H. Sánchez, L. M. Fernández, Sizing optimization, dynamic modeling and energy management strategies of a stand-alone pv/hydrogen/battery-based hybrid system, International Journal of Hydrogen Energy 38 (10) (2013) 3830 – 3845.

[26] N. Bizon, M. Oproescu, M. Raceanu, Efficient energy control strategies for a standalone renewable/fuel cell hybrid power source, Energy Conversion and Management 90 (2015) 93 – 110.

[27] M. Skoldstam, K. Akesson, M. Fabian, Modeling of discrete event systems using finite automata with variables, in: 2007 46th IEEE Conference on Decision and Control, 2007, pp. 3387–3392.

[28] P. J. G. Ramadge, W. M. Wonham, The control of discrete event systems, Proceedings of the IEEE 77 (1) (1989) 81–98.

[29] M. Skoldstam, K. Akesson, M. Fabian, Modeling of discrete event systems using finite automata with variables, in: 2007 46th IEEE Conference on Decision and Control, 2007, pp. 3387–3392. doi:10.1109/CDC.2007.4434894.

[30] J. Prosser, J. Selinsky, H. Kwatny, M. Kam, Supervisory control of electric power transmission networks, IEEE Transactions on Power Systems 10 (2) (1995) 1104–1110.

[31] M. S. Lee, J. T. Lim, Restoration strategy for power distribution networks using optimal supervisory control, IEE Proceedings-Generation, Transmission and Distribution 151 (3) (2004) 367–372.

[32] A. Afzalian, A. Saadatpoor, W. M. Wonham, Discrete-event system modeling and supervisory control for under-load tap-changing transformers, in: IEEE Conference on Computer Aided Control System Design, IEEE International Conference on Control Applications, IEEE International Symposium on Intelligent Control, 2006, pp. 1867–1872.

[33] A. A. Afzalian, S. A. N. Niaki, M. R. Iravani, W. M. Wonham, Discrete-event systems supervisory control for a dynamic flow controller, IEEE Transactions on Power Delivery 24 (1) (2009) 219–230.

[34] L. Feng, W. M. Wonham, Tct: A computation tool for supervisory control synthesis, in: 2006 8th International Workshop on Discrete Event Systems, 2006, pp. 388–389.

[35] A. Kharrazi, Y. Mishra, V. Sreeram, Discrete-event systems supervisory control for a custom power park, IEEE Transactions on Smart Grid PP (99) (2017) 1–1.

[36] J. Carroll, D. Long, Theory of finite automata with an introduction to formal languages, 1989.

[37] D. Giaouris, A. I. Papadopoulos, P. Seferlis, S. Voutetakis, S. Papadopoulou, Power grand composite curves shaping for adaptive energy management of hybrid microgrids, Renewable Energy 95 (2016) 433 – 448.

[38] M. F. Zia, E. Elbouchikhi, M. Benbouzid, Microgrids energy management systems: A critical review on methods, solutions, and prospects, Applied Energy 222 (2018) 1033 – 1055.

[39] M. Roslan, M. Hannan, P. J. Ker, M. Uddin, Microgrid control methods toward achieving sustainable energy management, Applied Energy 240 (2019) 583 – 607.

[40] Y. Khawaja, D. Giaouris, H. Patsios, M. Dahidah, Optimal cost-based model for sizing grid-connected pv and battery energy system, in: 2017 IEEE Jordan Conference on Applied Electrical Engineering and Computing Technologies (AEECT), 2017, pp. 1–6.

[41] N. Powergrid, Customer-led network revolution, https://www.petrolprices.com/the-price-of-fuel.html (Feb. 2018).

[42] M. Bortolini, M. Gamberi, A. Graziani, F. Pilati, Economic and environmental bi-objective design of an off-grid photovoltaic–battery–diesel generator hybrid energy system, Energy Conversion and Management 106 (2015) 1024 – 1038.

[43] NREL, Pvwatts calculator, /http://pvwatts.nrel.gov/ (Dec. 2017).

[44] R. Hosseinalizadeh, H. S. G, M. Amalnick, P. Taghipour, Economic sizing of a Hybrid (PV–WT–FC) Renewable Energy System (HRES) for Standalone Usages by an Optimization-Simulation Model: Case Study of Iran, Renewable and Sustainable Energy Reviews 54 (2016) 139 – 150.

[45] A. Mohammed, J. Pasupuleti, T. Khatib, W. Elmenreich, A review of process and operational system control of hybrid photovoltaic/diesel generator systems, Renewable and Sustainable Energy Reviews 44 (2015) 436 – 446.

[46] D. Giaouris, A. I. Papadopoulos, S. Voutetakis, S. Papadopoulou, P. Seferlis, A power grand composite curves approach for analysis and adaptive operation of renewable energy smart grids, Clean Technologies and Environmental Policy 17 (5) (2015) 1171–1193.

[47] D. Giaouris, A. I. Papadopoulos, P. Seferlis, S. Papadopoulou, S. Voutetakis, F. Stergiopoulos, C. Elmasides, Optimum energy management in smart grids based on power pinch analysis, CHEMICAL ENGINEERING 39.

[48] C. Wang, M. H. Nehrir, Power management of a stand-alone wind/photovoltaic/fuel cell energy system, IEEE Transactions on Energy Conversion 23 (3) (2008) 957–967.

[49] E. Eriksson, E. Gray, Optimization and integration of hybrid renewable energy hydrogen fuel cell energy systems - a critical review, Applied Energy 202 (2017) 348 – 364.

[50] O. Schmidt, A. Gambhir, I. Staffell, A. Hawkes, J. Nelson, S. Few, Future cost and performance of water electrolysis: An expert elicitation study, International Journal of Hydrogen Energy 42 (52) (2017) 30470 – 30492.

[51] M. Mehrpooya, M. Mohammadi, E. Ahmadi, Techno-economic-environmental study of hybrid power supply system: A case study in iran, Sustainable Energy Technologies and Assessments 25 (2018) 1 – 10.

[52] P. E. Campana, L. Wästhage, W. Nookuea, Y. Tan, J. Yan, Optimization and assessment of floating and floating-tracking pv systems integrated in on- and off-grid hybrid energy systems, Solar Energy 177 (2019) 782 – 795.

[53] A. Askarzadeh, Distribution generation by Photovoltaic and diesel generator systems: Energy management and size optimization by a new approach for a stand-alone application, Energy 122 (2017) 542 – 551.

[54] PetrolPrices, The price of fuel, https://www.petrolprices.com/the-price-of-fuel.html (Dec. 2017).

[55] T. Adefarati, R. Bansal, Reliability and economic assessment of a microgrid power system with the integration of renewable energy resources, Applied Energy 206 (2017) 911 – 933.

[56] T. Adefarati, R. Bansal, Reliability, economic, and enviromental analysis of a microgrid system in the presence of renewable energy resources, Applied Energy 236 (2019) 1089 – 1114.

[57] P. Zhou, R. Jin, L. Fan, Reliability and economic evaluation of power system with renewables: A review, Renewable and Sustainable Energy Reviews 58 (2016) 537 – 547.